

Prepared in cooperation with the U.S. Army Corps of Engineers

Use of Surrogate Technologies to Estimate Suspended Sediment in the Clearwater River, Idaho, and Snake River, Washington, 2008–10



Scientific Investigations Report 2013-5052

Cover:

Background: Confluence of the Snake and Clearwater Rivers at Lewiston, Idaho, May 14, 2012.

From left to right

Inset 1: Laser In Situ Scattering and Transmissometry (LISST)-Streamside laser diffraction instrument—Clearwater River at Spalding, Idaho, March 19, 2009.

Inset 2: Acoustic Doppler velocity meters (ADVMs)—Snake River near Anatone, Washington, March 20, 2009.

Inset 3: Nephelometric turbidity probe—Clearwater River at Spalding, Idaho, May 7, 2008.

All photographs were taken by Molly Wood, U.S. Geological Survey.

Use of Surrogate Technologies to Estimate Suspended Sediment in the Clearwater River, Idaho, and Snake River, Washington, 2008–10

By Molly S. Wood, U.S. Geological Survey, and Gregg N. Teasdale, U.S. Army
Corps of Engineers

Prepared in cooperation with the U.S. Army Corps of Engineers

Scientific Investigations Report 2013–5052

**U.S. Department of the Interior
U.S. Geological Survey**

U.S. Department of the Interior
KEN SALAZAR, Secretary

U.S. Geological Survey
Suzette M. Kimball, Acting Director

U.S. Geological Survey, Reston, Virginia: 2013

For more information on the USGS—the Federal source for science about the Earth, its natural and living resources, natural hazards, and the environment, visit <http://www.usgs.gov> or call 1–888–ASK–USGS.

For an overview of USGS information products, including maps, imagery, and publications, visit <http://www.usgs.gov/pubprod>

To order this and other USGS information products, visit <http://store.usgs.gov>

Any use of trade, firm, or product names is for descriptive purposes only and does not imply endorsement by the U.S. Government.

Although this information product, for the most part, is in the public domain, it also may contain copyrighted materials as noted in the text. Permission to reproduce copyrighted items must be secured from the copyright owner.

Suggested citation:
Wood, M.S., and Teasdale, G.N., 2013, Use of surrogate technologies to estimate suspended sediment in the Clearwater River, Idaho, and Snake River, Washington, 2008–10: U.S. Geological Survey Scientific Investigations Report 2013-5052, 30 p.

Contents

Abstract	1
Introduction.....	1
Background.....	3
Site Descriptions and Surrogate Instrument Configurations	4
Clearwater River Study Site	4
Snake River Study Site.....	6
Methods.....	8
Sediment Sample Collection.....	8
Surrogate Instrument Data Corrections	9
Acoustic Data Corrections	9
Acoustic Beam Spreading	9
Acoustic Absorption by Water	10
Acoustic Absorption by Sediment	11
Surrogate Model Development	11
Use of Surrogate Models To Estimate Suspended Sediment.....	12
Clearwater River Study Site	12
Snake River Study Site.....	18
Advantages of Acoustics over Sediment-Transport Curves in Sediment Monitoring	21
Comparison over Short Time Scales	21
Comparison over Annual Time Scales	26
Summary and Conclusions.....	27
Acknowledgments.....	27
References Cited.....	27

Figures

1. Map showing study area and locations of sediment surrogate and U.S. Geological Survey (USGS) streamgage sites in the Clearwater River, Idaho, and Snake River, Washington, May 2008–September 2010.....2
2. Photograph showing sediment surrogate instruments deployed at the Clearwater River near Spalding, Idaho.....5
3. Photographs showing sediment surrogate instruments deployed at the Snake River near Anatone, Washington.....6
4. Graph showing process for calculation of range-normalized acoustic backscatter corrected for two-way transmission losses in the Clearwater River, Idaho, and Snake River, Washington.....10
5. Graph showing surrogate regression models for total suspended sediment, sand, and fines concentrations based on acoustic backscatter for the Clearwater River near Spalding, Idaho
6. Graph showing measured and estimated total suspended sediment concentrations in the Clearwater River at Spalding, Idaho, based on a surrogate model with acoustic backscatter.....16

Figures—Continued

7. Graph showing estimated instantaneous values of total suspended-sediment concentration for March 23–July 1, 2010, in the Clearwater River near Spalding, Idaho, based on a surrogate model with acoustic backscatter and sediment-transport curves developed using data from the 2008–10 and 1970s studies	17
8. Graph showing surrogate regression models for total suspended sediment, sand, and fines concentrations based on acoustic backscatter for the Snake River near Anatone, Washington	18
9. Graph showing measured and estimated total suspended-sediment concentrations in the Snake River near Anatone, Washington, based on a surrogate model with acoustic backscatter	19
10. Graph showing estimated instantaneous values of suspended-sediment concentration during a storm event on June 1–15, 2010, in the Snake River near Anatone, Washington, based on a surrogate model with acoustic backscatter and sediment transport curves developed using data from the 2008–10 and 1970s studies	20
11. Boxplots showing distribution of total suspended-sediment concentration by month in the Clearwater River at Spalding, Idaho, based on (A) a surrogate model with 3MHz acoustic backscatter, (B) 2008–10 sediment transport curves, and (C) 1970s sediment transport curves, May 2008–September 2010	22
12. Graphs showing total suspended-sediment load by month based on a surrogate model with acoustic backscatter and 2008–10 and 1970s sediment-transport curves for the (A) Clearwater River at Spalding, Idaho, May 2008–September 2010, and (B) Snake River near Anatone, Washington, April 2009–September 2010	24

Tables

1. Suspended-sediment and streamflow data collected in the Clearwater River, Idaho, and Snake River, Washington, May 2008–September 2010	8
2. Surrogate model results and regression statistics for the Clearwater River at Spalding, Idaho, May 2008–September 2010	13
3. Surrogate model results and regression statistics for the Snake River near Anatone, Washington, May 2008–September 2010	14
4. Comparison of suspended sediment loads during selected storm events estimated using acoustic backscatter and sediment-transport curves based on 2008–10 streamflows in the Clearwater River at Spalding, Idaho, and Snake River near Anatone, Washington	25
5. Comparison of total, daily, and annual suspended sediment loads estimated using acoustic backscatter and sediment-transport curves based on 2008–10 and 1970s streamflows in the Clearwater River at Spalding, Idaho, and Snake River near Anatone, Washington	26

Conversion Factors and Datums

Conversion Factors

Inch/Pound to SI

Multiply	By	To obtain
Length		
foot (ft)	0.3048	meter (m)
mile (mi)	1.609	kilometer (km)
Area		
square mile (mi^2)	259.0	hectare (ha)
square mile (mi^2)	2.590	square kilometer (km^2)
Flow rate		
foot per second (ft/s)	0.3048	meter per second (m/s)
cubic foot per second (ft^3/s)	0.02832	cubic meter per second (m^3/s)
Mass		
ton, short (2,000 lb)	0.9072	megagram (Mg)
ton per day (ton/d)	0.9072	metric ton per day
ton per day (ton/d)	0.9072	megagram per day (Mg/d)
ton per year (ton/yr)	0.9072	megagram per year (Mg/yr)
ton per year (ton/yr)	0.9072	metric ton per year
Pressure		
atmosphere, standard (atm)	101.3	kilopascal (kPa)
pound-force per square inch (lbf/in ²)	6.895	kilopascal (kPa)
pound per square foot (lb/ft ²)	0.04788	kilopascal (kPa)
pound per square inch (lb/in ²)	6.895	kilopascal (kPa)

Conversion Factors and Datums—Continued

L Conversion Factors—Continued

SI to Inch/Pound

Multiply	By	To obtain
Length		
centimeter (cm)	0.3937	inch (in.)
meter (m)	3.281	foot (ft)
Volume		
liter (L)	33.82	ounce, fluid (fl. oz)
liter (L)	2.113	pint (pt)
liter (L)	1.057	quart (qt)
liter (L)	0.2642	gallon (gal)
liter (L)	61.02	cubic inch (in^3)
Flow rate		
centimeter per second (cm/s)	0.03281	foot per second (ft/s)
centimeter per second (cm/s)	0.03281	foot per second (ft/s)
Mass		
gram (g)	0.03527	ounce, avoirdupois (oz)
kilogram (kg)	2.205	pound avoirdupois (lb)
Density		
kilogram per cubic meter (kg/m^3)	0.06242	pound per cubic foot (lb/ft^3)
gram per cubic centimeter (g/cm^3)	62.4220	pound per cubic foot (lb/ft^3)

Temperature in degrees Celsius ($^{\circ}\text{C}$) may be converted to degrees Fahrenheit ($^{\circ}\text{F}$) as follows:

$$^{\circ}\text{F}=(1.8 \times ^{\circ}\text{C})+32.$$

Temperature in degrees Fahrenheit ($^{\circ}\text{F}$) may be converted to degrees Celsius ($^{\circ}\text{C}$) as follows:

$$^{\circ}\text{C}=(^{\circ}\text{F}-32)/1.8.$$

Datums

Vertical coordinate information is referenced to the North American Vertical Datum of 1988 (NAVD 88).

Horizontal coordinate information is referenced to the North American Datum of 1983 (NAD 83).

Altitude, as used in this report, refers to distance above the vertical datum.

Use of Surrogate Technologies to Estimate Suspended Sediment in the Clearwater River, Idaho, and Snake River, Washington, 2008–10

By Molly S. Wood, U.S. Geological Survey, and Gregg N. Teasdale, U.S. Army Corps of Engineers

Abstract

Elevated levels of fluvial sediment can reduce the biological productivity of aquatic systems, impair freshwater quality, decrease reservoir storage capacity, and decrease the capacity of hydraulic structures. The need to measure fluvial sediment has led to the development of sediment surrogate technologies, particularly in locations where streamflow alone is not a good estimator of sediment load because of regulated flow, load hysteresis, episodic sediment sources, and non-equilibrium sediment transport. An effective surrogate technology is low maintenance and sturdy over a range of hydrologic conditions, and measured variables can be modeled to estimate suspended-sediment concentration (SSC), load, and duration of elevated levels on a real-time basis. Among the most promising techniques is the measurement of acoustic backscatter strength using acoustic Doppler velocity meters (ADVMs) deployed in rivers. The U.S. Geological Survey, in cooperation with the U.S. Army Corps of Engineers, Walla Walla District, evaluated the use of acoustic backscatter, turbidity, laser diffraction, and streamflow as surrogates for estimating real-time SSC and loads in the Clearwater and Snake Rivers, which adjoin in Lewiston, Idaho, and flow into Lower Granite Reservoir. The study was conducted from May 2008 to September 2010 and is part of the U.S. Army Corps of Engineers Lower Snake River Programmatic Sediment Management Plan to identify and manage sediment sources in basins draining into lower Snake River reservoirs.

Commercially available acoustic instruments have shown great promise in sediment surrogate studies because they require little maintenance and measure profiles of the surrogate parameter across a sampling volume rather than at a single point. The strength of acoustic backscatter theoretically increases as more particles are suspended in the water to reflect the acoustic pulse emitted by the ADVM. ADVMs of different frequencies (0.5, 1.5, and 3 Megahertz) were tested to target various sediment grain sizes. Laser diffraction and turbidity also were tested as surrogate technologies. Models between SSC and surrogate variables were developed using ordinary least-squares regression. Acoustic backscatter using

the high frequency ADVM at each site was the best predictor of sediment, explaining 93 and 92 percent of the variability in SSC and matching sediment sample data within +8.6 and +10 percent, on average, at the Clearwater River and Snake River study sites, respectively. Additional surrogate models were developed to estimate sand and fines fractions of suspended sediment based on acoustic backscatter. Acoustic backscatter generally appears to be a better estimator of suspended sediment concentration and load over short (storm event and monthly) and long (annual) time scales than transport curves derived solely from the regression of conventional sediment measurements and streamflow. Changing grain sizes, the presence of organic matter, and aggregation of sediments in the river likely introduce some variability in the model between acoustic backscatter and SSC.

Introduction

The U.S. Geological Survey (USGS) Idaho Water Science Center, in cooperation with the U.S. Army Corps of Engineers (USACE), Walla Walla District, is evaluating surrogate technologies to estimate suspended-sediment concentrations (SSC) in the Clearwater River at Spalding, Idaho, and the Snake River near Anatone, Washington ([fig. 1](#)) to help quantify sediment transport to Lower Granite Reservoir in northern Idaho and eastern Washington. USACE is developing strategies for managing fluvial sediment transport and deposition in lower Snake River reservoirs, which has negatively affected navigation and flow conveyance. Historically, sediment deposition has been managed through periodic dredging of the federal navigation channel; however, USACE plans to identify more opportunities for controlling sediment by quantifying sediment sources and transport in contributing drainage basins, particularly the Clearwater, Snake, and Salmon River basins. Streamflow in the two river systems is partially regulated, meaning that some but not all of the flow is controlled by dam releases. Some flow passing each study site is contributed by unregulated (free-flowing) tributaries.

2 Surrogate Technologies to Estimate Suspended Sediment, Clearwater River, Idaho, and Snake River, Wash., 2008–10

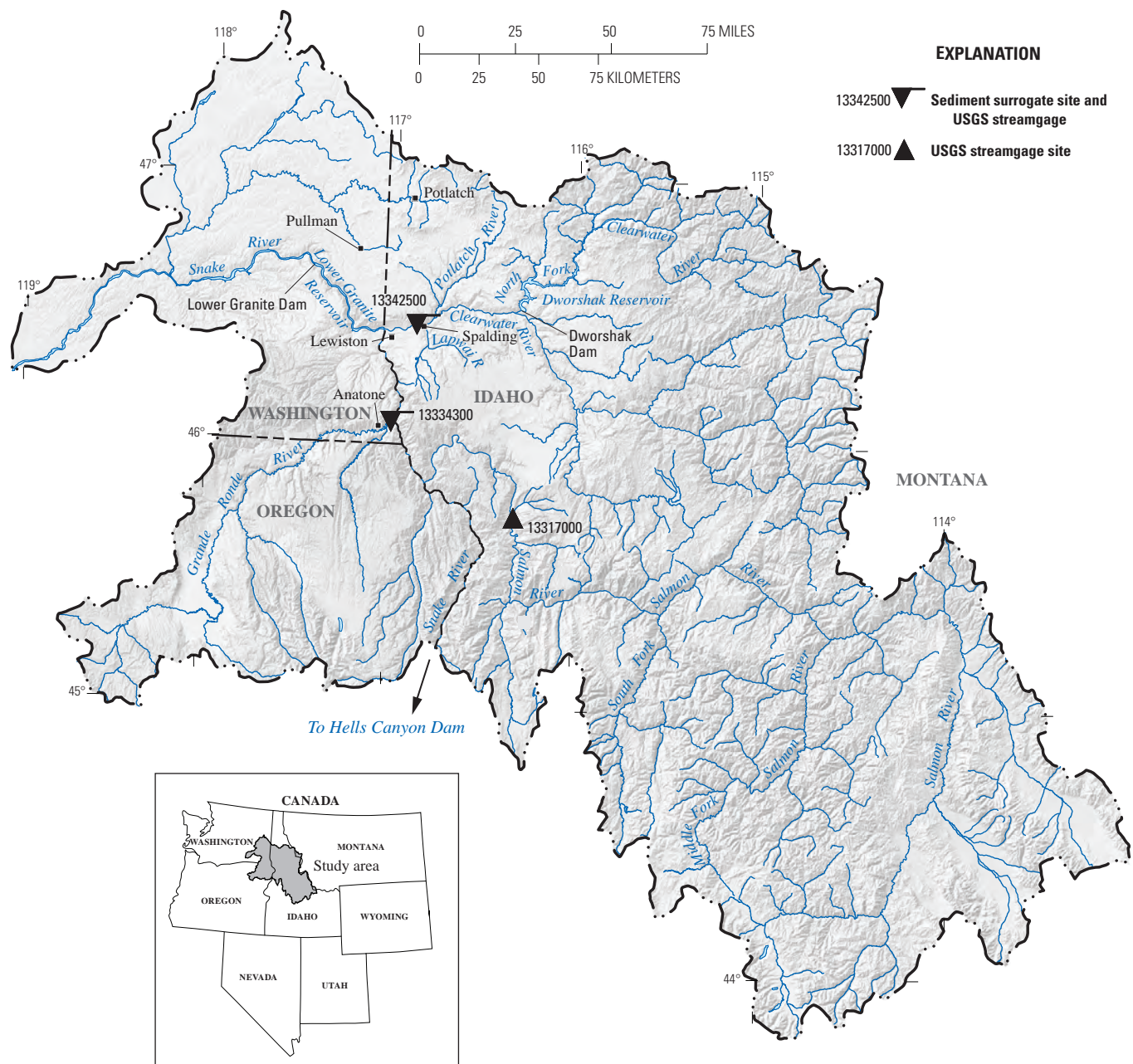


Figure 1. Study area and locations of sediment surrogate and U.S. Geological Survey (USGS) streamgage sites in the Clearwater River, Idaho, and Snake River, Washington, May 2008–September 2010.

The Lower Granite Lock and Dam forms the farthest upstream reservoir on the lower Snake River and captures sediment from about 27,000 mi² of forested and agricultural land in the Clearwater, Salmon, and Grande Ronde River basins (Teasdale, 2010). Levees were constructed along the Snake and Clearwater Rivers in Lewiston, Idaho, to contain the backwater of Lower Granite Dam and provide flood damage reduction up to the level of the Standard Project Flood, which is the streamflow expected to result from the most severe hydrologic and meteorological conditions that is characteristic of the drainage basins (U.S. Army Corps of Engineers, 2002). Sediment deposition has reduced the hydraulic capacity of the levees since completion of the dam in 1974. Periodic dredging has been performed by the USACE to maintain the navigation channel and recover hydraulic capacity of the levee system. An Environmental Impact Statement (EIS) for proposed dredging action prepared by the USACE in 2002 was suspended in litigation and the USACE is now revising the EIS as part of the development of a comprehensive Programmatic Sediment Management Plan (PSMP). The PSMP-EIS is evaluating alternatives to dredging, including drainage basin measures that may reduce sediment loads and the construction of structures within the reservoir to promote movement of sediment through the confluence. Accurate measurements of sediment concentration and load are necessary to plan and evaluate potential sediment management actions and to calibrate sediment yield and transport models.

The USGS conducted a sediment sampling program in the Clearwater and Snake Rivers from 1972 to 1979 and developed sediment-transport curves that related streamflow to suspended and bedload sediment samples to calculate continuous records of sediment concentration and load. The results of the 1970s study are presented in Jones and Seitz (1980). One of the goals of the 2008–10 sediment sampling program was to determine whether the 1970s sediment-transport curves are representative of current sediment-transport conditions. A detailed discussion of comparisons between results of the 1970s and 2008–10 sampling programs is provided in Clark and others (2013).

This report documents the ability and limitations of using sediment-surrogate technologies (surrogate technologies), such as acoustic backscatter, laser diffraction, and turbidity, to estimate SSC and load on continuous, 15-min intervals in the Snake and Clearwater Rivers draining to Lower Granite Reservoir. Surrogate technologies are evaluated to determine whether they provide improved estimates of SSC and load in comparison with sediment-transport curves generated using streamflow and sediment data collected during the 1970s and 2008–10 studies. Transport curves relying on streamflow as the explanatory variable may be poor estimators of SSC in these river systems, particularly during rain events, owing to “hysteresis” and varying sources of sediment (mostly from unregulated tributary inflows) that may not contribute a large percentage of the total flow but contribute a large amount

of sediment. Sediment “hysteresis” means that sediment concentrations have different values at identical streamflow on the ascending and descending limbs of a hydrograph. A plot of streamflow and SSC during a storm event often appears to have a looped relation owing to hysteresis.

Additional sediment samples and surrogate data were collected in water year 2011 to validate the acoustic backscatter surrogate models described in this report; validation results are presented in Clark and others (2013). Clark and others (2013) also presents a comparison of suspended sediment-load estimates generated using the acoustic backscatter surrogate models described in this report and using a LOADEST (LOAD ESTimation) model, which is a FORTRAN (FORmula TRANslatIOn) program for estimating constituent loads in streams and rivers based on streamflow and time variables (Runkel and others, 2004).

Background

The USGS has traditionally used streamflow as a surrogate to estimate instantaneous SSC and sediment loads based on guidelines in Porterfield (1972), Glysson (1987), and Nolan and others (2005). A relation is developed between streamflow and SSC or sediment load using log transformations on both variables or plotting on logarithmic scales. The relation, which may be linear or non-linear, is called a sediment-transport curve.

Uncertainties in sediment-transport curves have led to the development and evaluation of more direct, in-situ surrogate techniques. Acoustic instruments have shown great promise as sediment- surrogate technologies. They are tolerant of biological fouling and measure profiles across a sampling volume rather than at a single point in the stream (Gartner and Gray, 2005).

Acoustic backscatter has been used with success as a surrogate technology for SSC or suspended solids concentration in the San Francisco Bay (Gartner, 2004), Florida estuaries (Patino and Byrne, 2004), Colorado River (Topping and others, 2004, 2006), Hudson River (Wall and others, 2006), the Aegean Region in Turkey (Elci and others, 2009), and subtropical estuaries in Australia (Chanson and others, 2008). Although the primary purpose of these types of acoustic instruments is to measure water velocity, additional measures are useful to monitor suspended-sediment transport. As the instrument emits an acoustic pulse into the water and measures the Doppler-shifted frequency of the pulse as it bounces off acoustic reflectors (typically assumed to be primarily sediment particles), the strength of the returned pulse (backscatter) also is measured as it returns to the instrument along the beam path (SonTek/Yellow Springs Instruments, 2007). Backscatter should increase when more particles are present in the water. As a result, the backscatter measurement may be related to SSC.

Additional surrogate technologies have been used to monitor suspended-sediment transport. Turbidity has been successfully used as a surrogate for SSC in Kansas (Rasmussen and others, 2005), Oregon (Uhrich and Bragg, 2003), and Florida (Lietz and Debiak, 2005), among other locations. Turbidity probes typically used in these studies emit a near-infrared light at 780–900 nm and measure the amount of light scattered at an angle of 90 degrees (Yellow Springs Instruments, 2011). The greater the amount of light scattered, the higher the turbidity reading. In theory, this should equate to a larger amount of suspended material in the measurement volume.

The concept of laser diffraction is documented in Agrawal and others (2008) and has been used with success as a sediment surrogate in the Colorado River (Topping and others, 2004) and in laboratory experiments (Meral, 2008). Essentially, a laser is passed through a water sample and a receiving lens in the instrument focuses the light that is scattered by particles in the water onto a series of ring detectors. The detectors calculate a volumetric concentration of sediment in 32 size classes. Data can be converted to a mass concentration by multiplying the volumetric concentration by a known sediment density, or the volumetric concentrations can be used alone in a calibration with measured SSC.

Site Descriptions and Surrogate Instrument Configurations

Study sites were co-located with existing USGS streamgages to take advantage of existing infrastructure for mounting equipment and transmitting data and to facilitate computations of sediment loads. Acoustic frequencies were selected for this study to maximize sensitivity of backscatter to dominant sediment particle size (grain size) with low acoustic frequency for the sand-sized fraction (grain size between 0.63 and 2 mm) and high acoustic frequency for the fines fraction (grain size less than 0.63 mm) to minimize errors because of changing grain-size distribution, as recommended in Gartner (2004) and Topping and others (2004). The following sections describe characteristics of the two study sites and configuration of surrogate instruments.

Clearwater River Study Site

The Clearwater River study site is co-located with USGS streamgage No. 13342500 on the left streambank at Spalding, Idaho. Part of the streamflow passing the study site is regulated by Dworshak Dam located upstream of the site on the North Fork Clearwater River ([fig. 1](#)). The main stem Clearwater River is unregulated except for a few upstream

irrigation diversions, which affect about 18 percent of the drainage area (U.S. Geological Survey, 2012). The site is equipped with a 0.5-MHz SonTek™/YSI Argonaut-SL acoustic Doppler velocity meter (ADVM), a 3-MHz SonTek™/YSI Argonaut-SL ADVM, a Yellow Springs Instruments (YSI™) 6600EDS water-quality sonde with a model 6136 nephelometric turbidity probe, and a Sequoia Scientific Laser In Situ Scattering and Transmissometry (LISST)-StreamSide laser diffraction instrument ([fig. 2](#)). The YSI™ 6136 nephelometric turbidity probe used in this study emits a near-infrared light at 780–900 nm and measures the amount of light scattered at an angle of 90 degrees (Yellow Springs Instruments, 2011). The site also is equipped with a datalogger and satellite telemetry for collecting and transmitting real-time data. The ADVMs, turbidity probe, and telemetry were installed in May 2008; the LISST-StreamSide was installed in July 2008. The LISST-StreamSide is deployed inside a gage house, and a pump draws water from the river into the LISST-StreamSide optical analyzer box. The intended advantage of the LISST-StreamSide over other commercially available, in-situ laser diffraction instruments as described in Gray and Gartner (2010) is improved data quality through reduced stream contact and resulting biological fouling. Unforeseen configuration problems in the LISST-StreamSide, which resulted in poor pump operation, the formation of bubbles in the line, and possible condensation on internal lenses, prevented reliable measurements for most of the study period. The manufacturer of the LISST-StreamSide, Sequoia Scientific, is working closely with the USGS to resolve the problems. Further testing is needed to determine whether the instrument will perform as intended, once these issues are resolved.

The ADVMs, turbidity probe, and LISST-StreamSide pump intake are mounted on a 44-ft aluminum slide-track mount that can be raised and lowered as needed to service equipment. The 0.5- and 3-MHz ADVMs measure backscatter in five discrete, equally sized cells in a horizontal sampling volume, at distances of 5.0–100 ft and 3.3–12 ft from the instrument, respectively. The sampling volume for each ADVM was selected based on acoustic frequency, abundance of acoustic reflectors along the beam path, and any obstructions in the beam path. The ADVMs were originally configured to measure backscatter in 10 cells, within a sampling volume twice as large as the current configuration. However, the sampling volume represented by the first five cells was determined to be optimum for developing the model between SSC and acoustic backscatter. In addition, data transfer limitations using Serial Data Interface-1200 baud rate (SDI-12) protocol, the communication protocol used to transfer data from the ADVMs to the dataloggers at both sites, prevents real-time display of data from more than five cells. As a result, only the first five cells could be practically used to compute real-time estimates of SSC and sediment load using developed surrogate models.



Figure 2. Sediment surrogate instruments deployed at the Clearwater River near Spalding, Idaho. Instruments are shown pulled up the slide track mount for servicing. Not shown: the pump and intake for the LISST-StreamSide was later installed on the back side of the aluminum plate attached to the acoustic Doppler velocity meters. Photograph taken by Molly Wood, U.S. Geological Survey, May 8, 2009.

The ADVMs average measurements collected over 2 min out of every 15 min. The water-quality sonde measures turbidity adjacent to the instrument every 15 min and is equipped with an automated wiper mechanism to reduce biological fouling on the face of the probe. The LISST-StreamSide measures volumetric SSC and grain-size distribution every 30 min. The sampling line for the LISST-StreamSide is flushed for 2–5 min prior to each measurement (duration changed during study period), and measurements are then averaged over 30 sec.

Snake River Study Site

The Snake River study site is co-located with USGS streamgage No. 13334300 on the left streambank near Anatone, Washington ([fig. 1](#)). Part of the streamflow passing the study site is regulated by numerous dams along the Snake River, including Hells Canyon Dam located 31 mi upstream. The Salmon and Grande Ronde Rivers join the Snake River upstream of the study site and contribute most of the sediment passing the site (Gregory Clark, U.S. Geological Survey, oral commun., 2011). The site is equipped with a 0.5-MHz SonTek™/YSI Argonaut-SL ADVM, a 1.5-MHz SonTek™/YSI Argonaut-SL ADVM, and a YSI™ 6600EDS water-quality sonde with a model 6136 turbidity probe ([fig. 3](#)).



A. The pipe housing a Yellow Springs Instruments (YSI™) water-quality sonde with turbidity probe.

Figure 3. Sediment surrogate instruments deployed at the Snake River near Anatone, Washington. (Photographs *A* and *B* taken December 15, 2008 and March 30, 2009, respectively, by Molly Wood, U.S. Geological Survey.)



B. The 1.5-MHz and 0.5-MHz SonTek™/YSI acoustic Doppler velocity meters (ADVMs) attached to an aluminum slide track mount about 1,000 ft upstream of the water-quality sonde.

Figure 3.—Continued

Like the Clearwater River study site, the Snake River site is equipped with a datalogger and satellite telemetry. The water-quality sonde and telemetry were installed in May 2008; the ADVMs were installed in April 2009. The water-quality sonde is mounted in a plastic pipe, drilled with holes to maintain hydraulic communication between the inside of the pipe and surrounding water, which extends into the river from the left bank near the gage house. The ADVMs could not be co-located with the streamgage and water-quality sonde because streambed

features limited profiling across the channel. The ADVMs were installed in a more suitable measurement location about 1,000 ft upstream of the streamgage, on a 32-ft aluminum slide track mount that can be raised and lowered as needed to service the equipment.

The 0.5- and 1.5-MHz ADVMs are configured to measure backscatter in five discrete, equally sized cells in a horizontal sampling volume, 6.6–203 ft and 6.6–59 ft from the instrument, respectively. The ADVMs average measurements collected over 2 min out of every 15 min. The water-quality sonde measures turbidity adjacent to the instrument every 15 min and is equipped with an automated wiper mechanism.

Unlike the Clearwater River site, the ADVMs at the Snake River site are direct current-powered through a solar panel and battery. To avoid fluctuations in input voltage, which is common at sites powered by a solar panel and battery, that could lead to fluctuations in power during transmission of the acoustic pulse (Craig Huhta, SonTek/Yellow Springs Instruments, oral commun., 2012), both ADVMs are connected to a direct current voltage converter to maintain a constant voltage input to the instruments during measurements. The voltage converter changes direct current voltage from a solar panel and battery to a constant output of 13 volts to the ADVMs, to remove the potential uncertainty in backscatter measurements because of fluctuations in input voltage. This setup was deemed necessary because Wall and others (2006) noted that differing power-supply voltages supplied to acoustic Doppler current profilers used to estimate sediment in the Hudson River resulted in changes in transmit power of the acoustic pulse, which required corrections to the data. This phenomenon could cause fluctuations in backscatter measurements which are not a result of changes in SSC in the river.

Methods

The following sections describe the methods used to collect suspended-sediment samples, process and apply corrections to surrogate data, and develop surrogate models for the computation of continuous records of SSC and load.

Sediment Sample Collection

Suspended-sediment samples were collected using the equal-width-increment (EWI) sampling method (U.S. Geological Survey, 2006) with a cable-suspended, US D-96 depth-integrating, isokinetic water sampler and were analyzed at the USGS Cascades Volcano Observatory Sediment Laboratory in Vancouver, Washington. Sampling was targeted towards the ascending limb, the peak, and the descending limb of the snowmelt runoff hydrograph for each river. Thirty-three EWI suspended-sediment samples were collected at each site during May 2008–September 2010 ([table 1](#)) and were analyzed for concentration, percent fines smaller than 0.063 mm, and organic content through a loss-on-ignition test. A full grain-size analysis on the sand fraction was performed for some samples. Samples submitted for analysis were a composite representative of the entire cross section.

To quantify cross-sectional variability, 10 discrete depth-integrated samples, each from a separate vertical section, were collected and analyzed during 4 sampling events at the Clearwater River site and 5 sampling events at the Snake River site. EWI samples should have been collected with

each of the discrete sample subsets because the average concentration from the discrete sample subsets may not necessarily equal the EWI sample concentration. However, EWI samples were collected concurrently for only two of the discrete sample subsets at the Snake River site. When discrete bottles were collected without a corresponding EWI sample, the results from the discrete samples were averaged for use in the analysis. Discrete and corresponding EWI samples were collected at flows of 48,000 and 105,000 ft³/s at the Snake River site. Ratios were calculated between the EWI sample concentration and average concentration from discrete samples for these two sampling events. The ratios were 0.79 and 0.96 for the higher and lower flow sampling events, respectively, meaning that in both cases the EWI sample concentration was less than the average concentration from discrete samples. Sample results from the remaining three sampling events in the Snake River, when a corresponding EWI sample was not collected, were adjusted based on these ratios. Samples collected at 24,600 and 55,000 ft³/s were adjusted using the 0.96 (lower flow) ratio and a sample collected at 103,000 ft³/s was adjusted using the 0.79 (higher flow) ratio. For example, the average concentration for discrete samples collected on May 20, 2009, at a flow of 103,000 ft³/s was 301 mg/L. The concentration was adjusted to $301 \text{ mg/L} \times 0.79 = 237 \text{ mg/L}$ to estimate what the EWI sample concentration might have been for that sampling event. None of the samples on the Clearwater River site were adjusted in this way because no corresponding EWI samples were collected concurrently with the four discrete sample subsets.

Table 1. Suspended-sediment and streamflow data collected in the Clearwater River, Idaho, and Snake River, Washington, May 2008–September 2010.

[Abbreviations: USGS, U.S. Geological Survey; mg/L, milligrams per liter; ft³/s, cubic feet per second; na, not applicable]

Characteristic	USGS streamgage		Units
	Clearwater River (13342500)	Snake River (13334300)	
Number of sediment samples collected during study period	33	33	na
Mean annual streamflow, period of record ¹	14,710	34,450	ft ³ /s
Annual mean streamflow			
2008	16,220	31,310	ft ³ /s
2009	16,040	33,080	ft ³ /s
2010	10,830	29,130	ft ³ /s
Total suspended-sediment concentration			
Mean	26	70	mg/L
Median	13	40	mg/L
Ranges			
Total suspended-sediment concentration	3–210	6–414	mg/L
Sand concentration	0.3–122	0.5–232	mg/L
Fines concentration	2–88	5–206	mg/L
Flows during sample collection	4,760–78,900	14,900–155,000	ft ³ /s
Flows during study period (May 2008–September 2010)	2,190–79,700	10,900–173,000	ft ³ /s

¹ Based on published period of record for streamgage, water years 1972–2010 for Clearwater River, 1958–2010 for Snake River.

Surrogate Instrument Data Corrections

The surrogate technologies required varying levels of correction to be used in SSC estimates from the raw measured values. Turbidity data were corrected for calibration drift and fouling errors as described in Wagner and others (2006). Laser diffraction data were recorded by the instrument in volumetric concentration in microliters per liter ($\mu\text{L/L}$), which can be multiplied by a known or assumed particle density to obtain mass concentration in milligrams per liter (mg/L). In this investigation, it was not practical to continuously measure particle density, so a regression model was developed between LISST volumetric concentration and the mass concentration of the physical samples. No corrections were applied to the LISST volumetric concentration data.

To correct acoustic backscatter data into a more meaningful estimator of SSC, multiple steps are required. Acoustic backscatter data were corrected for (1) beam spreading, (2) transmission losses owing to absorption by water, and (3) absorption or attenuation by sediment. Methods for correcting acoustic backscatter data are documented in Flammer (1962), Urick (1975), Thevenot and Kraus (1993), and Gartner (2004). Methods for correcting acoustic backscatter data differ and can significantly change estimates of sediment concentration. Selection of an appropriate method is an important decision in the analysis of acoustic backscatter data. Candidate methods were reviewed and those selected for this study are described in the following sections.

Acoustic Data Corrections

Mass concentration of suspended sediment can be related to acoustic backscatter using equation (1) in exponential form:

$$\text{SSC} = 10^{(\beta_0 + (\beta_1 \text{ABS}_{\text{corr}}) + (\beta_2 EVi) + \dots + (\beta_n EVn))} \quad (1)$$

where

SSC is suspended-sediment concentration (mg/L)
 β_0 is the equation intercept,
 β_1 is the regression coefficient corresponding to ABS_{corr} , and
 ABS_{corr} is the range-normalized acoustic backscatter (ABS) corrected for two-way transmission losses (Thevenot and Kraus, 1993) in decibels (dB).

EVi through EVn are other explanatory variables used in the regression, and β_2 through β_n are the corresponding regression coefficients. The regression coefficients are determined by regressing mass concentration measurements of suspended sediment with measurements of ABS_{corr} and other explanatory variables during sample collection.

Backscatter data must be range-normalized or corrected for transmission losses through a multi-step process (fig. 4).

Corrected acoustic backscatter, ABS_{corr} , is calculated using a form of the sonar equation from Urick (1975):

$$\text{ABS}_{\text{corr}} = K(E - E_r) + 20 \log_{10}(R) + 2\alpha_w R + 2\alpha_s R \quad (2)$$

where

ABS_{corr} is the range-normalized acoustic backscatter corrected for two-way transmission losses in dB,
 K is a scale factor used to convert uncorrected ABS in counts to dB,
 E is the raw amplitude of the uncorrected ABS as reported by the acoustic device (counts),
 E_r is the received signal strength indicator reference level or instrument noise floor (counts),
 R is the slant distance along the acoustic beam to the measurement location incorporating beam angle (25 degrees for SonTek™/YSI ADVMs) (m),
 α_w is the water absorption coefficient (dB/m), and
 α_s is the sediment attenuation coefficient (dB/m).

The scale factor used to convert uncorrected ABS in counts to dB typically ranges from 0.35 to 0.55 according to Deines (1999). For SonTek™/YSI ADVMs, the appropriate value for K when converting ABS from counts to dB is 0.43 (SonTek/Yellow Springs Instruments, 2007). The term E_r , or instrument noise floor, is specific to the ADVM and deployment location, and is the baseline echo measured by the instrument when no signal is transmitted. Local electronic interferences can affect E_r . E_r is measured automatically by the ADVMs used in this study immediately after a backscatter measurement is made. The term $K(E - E_r)$ is output from the SonTek™/YSI ADVMs directly as Signal to Noise Ratio (SNR) in each cell, so this term was used in all calculations because it incorporated actual measurements of the instrument noise floor (fig. 4, step 1).

Acoustic Beam Spreading

Losses owing to beam spreading, represented by the term $20 \log_{10}(R)$ in equation (2), are different for acoustic backscatter data collected near the transducer, or within a zone called the near-field distance. The near-field distance is defined by $R_{\text{critical}} = \pi r_t^2 / \lambda$, where r_t is the transducer radius (cm) and λ is the acoustic wavelength, or the speed of sound in water (cm/s) divided by the acoustic frequency (Hz). At distances less than R_{critical} , the near-field correction for spreading loss is defined by Downing and others (1995) as:

$$\Psi = \left[1 + 1.35Z + (2.5Z)^{3.2} \right] / \left[1.35Z + (2.5Z)^{3.2} \right] \quad (3)$$

where

$Z = R/R_{\text{critical}}$ and R is the slant range distance along the beam to the sampling volume of interest.

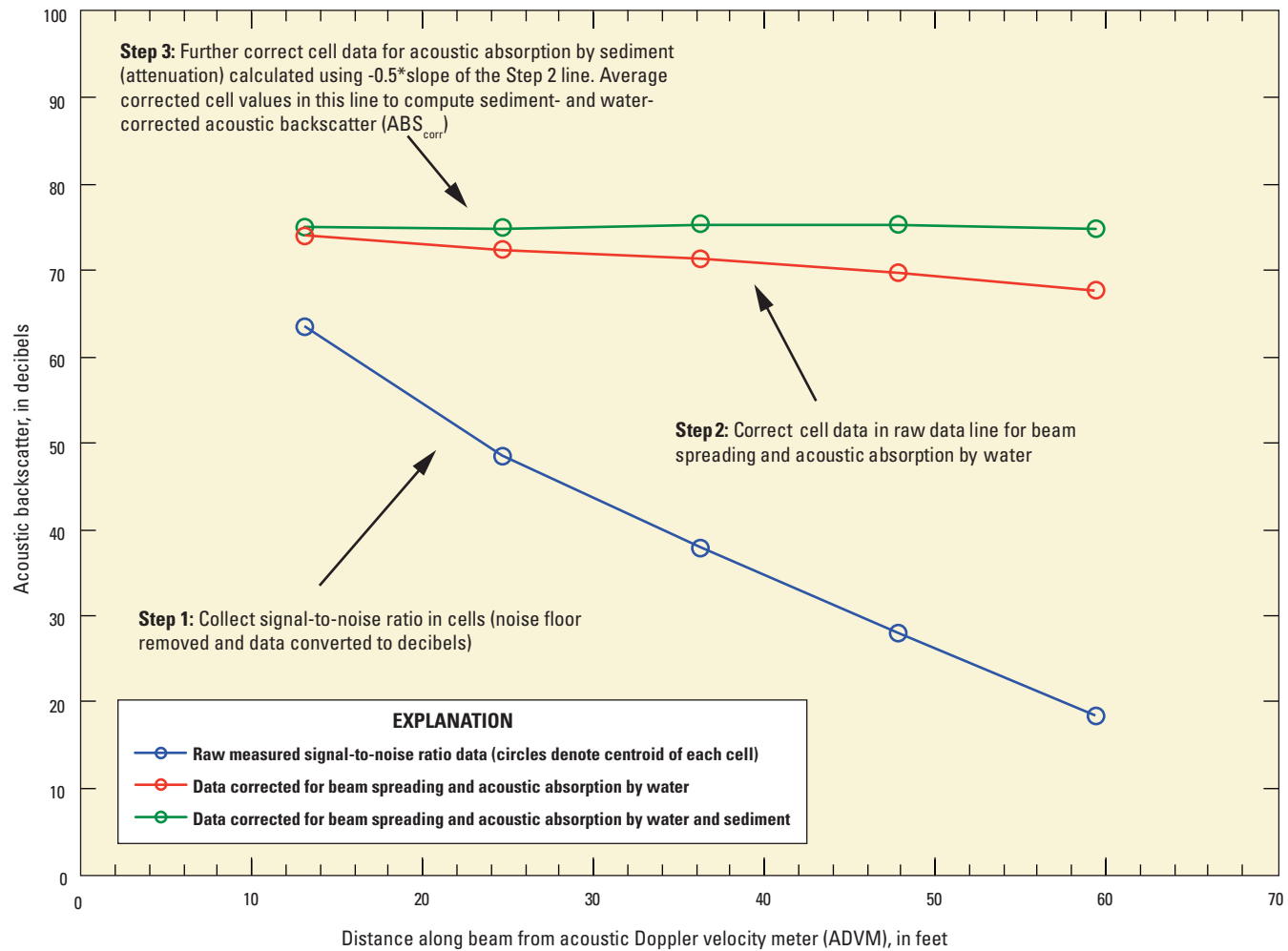


Figure 4. Process for calculation of range-normalized acoustic backscatter corrected for two-way transmission losses in the Clearwater River, Idaho, and Snake River, Washington.

At points within the near field, the term $20\log_{10}(R)$ in equation (2) becomes $20\log_{10}(R\Psi)$. Cell 1 centroids for the ADVMs in the Clearwater and Snake Rivers were greater than $R_{critical}$ and so were not corrected for near-field spreading losses. Losses owing to beam spreading were calculated simply using the term $20\log_{10}(R)$.

Acoustic Absorption by Water

The water absorption coefficient, α_w , in equation (2) is a function of acoustic frequency, pressure, salinity, and temperature; and is calculated according to Schulkin and Marsh (1962):

$$\alpha_w = [SAf_t f^2 / (f_t^2 + f^2) + Bf^2 / f_t] \quad (4)$$

$$[1 - (6.54 \times 10^{-4})(P)] \times 8.686$$

where

α_w is the water absorption coefficient (dB/m),
 S is salinity (practical salinity units),

A is a constant for ionic relaxation process in sea water equal to 2.34×10^{-6} ,
 f_t is the temperature-dependent relaxation frequency (kilohertz or kHz) defined as $21.9 \times 10^{[6-1520/(T+273)]}$,
 T is temperature ($^{\circ}\text{C}$),
 f is the ADVM acoustic frequency (kHz),
 B is a constant for viscosity mechanism in pure water, defined as 3.38×10^{-6} , and
 P is pressure (atmospheres or kg/cm^3).

In this analysis, the first term of the equation, $SAf_t f^2 / (f_t^2 + f^2)$, is assumed to be zero because salinity is negligible. Pressure, P , is considered 1 atmosphere because the difference in pressure between the elevations of the water surface at the sites (about 800 ft above sea level) and the depth of the deployed ADVMs is negligible.

The terms $20\log_{10}(R)$ and $2\alpha_w R$ in equation (2) represent the two-way transmission loss, or acoustic signal loss owing to beam spreading and acoustic absorption by water. Data corrected for these losses are represented by step 2 in [figure 4](#).

Acoustic Absorption by Sediment

The last term in equation (2), $2\alpha_s R$, represents the two-way transmission loss owing to absorption or attenuation by sediment, and ideally should be calculated based on knowledge of source level, target strength, ensonified volume, and mass of suspended material in various size classes. Attenuation of an acoustic signal by suspended particles consists of viscous, scattering, and diffraction energy loss components (Flammer, 1962). Diffraction losses are described in more detail in Reichel and Nachtnebel (1994) and are not a concern at the study site, given the frequency of the selected ADVMs and measured sediment concentrations and particle sizes. A theoretical calculation of viscous and scattering losses can be made based on the following equation from Urick (1975):

$$2\alpha_s = \underbrace{(K(\gamma-1)^2 \{S / [S^2 + (\gamma+\tau)^2]\})}_{\text{Viscous losses}} + \underbrace{(K^4 a_p^3 / 6)(8.686)(SSC)}_{\text{Scattered losses}} \quad (5)$$

where

- SSC is the suspended-sediment concentration (mg/L)
- $2\alpha_s$ is the two-way transmission loss owing to attenuation from suspended particles (dB/m),
- K is $2\pi/\lambda$,
- λ is acoustic wavelength or the speed of sound in water (cm/s) divided by acoustic frequency (Hz),
- S is $[9/(4\beta a_p)][1+1/(\beta a_p)]$, β is $[\omega/2v]^{0.5}$, ω is $2\pi f$,
- f is acoustic frequency (Hz),
- v is the kinematic viscosity of water (Stokes),
- a_p is particle radius (cm),
- γ is the particle wet density divided by fluid density, and
- τ is $0.5+9/(4\beta a_p)$.

It was not always practical to measure true values for some of the parameters in equation (5) given the expected non-uniformity in particle shape, size, and density. Topping and others (2004, 2006) proposed that the acoustic absorption by sediment (attenuation) can be calculated based on profiles of acoustic backscatter corrected for spherical beam spreading and absorption by water. In Topping and others (2004, 2006) and the study reported here, $2\alpha_s R$ in equation (2) was calculated for each cell by determining -0.5 times the slope of the line of $K(E-E_r)+20\log_{10}(R)+2\alpha_w R$ (represented by the line in [fig. 4](#), step 2). This value, called sediment attenuation, or α_s , is then multiplied by $2\times R$ (the slant range distance along the beam to the sampling volume of interest). ABS_{corr} was then calculated for each cell according to equation (2) ([fig. 4](#), step 3), and the average of ABS_{corr} from all cells was used to relate surrogate data to sediment sample data.

During some brief periods of low backscatter and low SSC, the line representing data corrected for beam spreading and acoustic absorption by water ([fig. 4](#), step 2) curved upward in cells 4 or 5. This is not physically possible, and use of this data in the

calculations would have resulted in erroneous estimates of the slope of the line, or sediment attenuation. During these periods, acoustic backscatter in the outer cell(s) may have been erroneous because it could not be distinguished from the instrument noise floor. When this occurred, these cells were discarded from the calculation of sediment attenuation. Only cells along the decreasing trend of the line representing data corrected for beam spreading and acoustic absorption by water were used to calculate sediment attenuation for further correction of the data in step 3 of [figure 4](#).

Surrogate Model Development

Samples collected in 2008–10 were used to develop sediment-surrogate models at each site. Surrogate measurements (acoustic backscatter, turbidity, streamflow, and laser diffraction (laser diffraction was measured at the Clearwater River site but not the Snake River site) data) were averaged over a 1-hour period bracketing each sediment sample to obtain concurrent measurements for surrogate-model calibrations. Some samples were not included in the surrogate models because of intermittent equipment malfunctions, varying installation dates for surrogate instruments, and surrogate instruments being out of water for short periods of time during low-flow conditions.

Models between SSC and surrogate variables were developed using stepwise ordinary least-squares regression techniques in TIBCO Spotfire S+® statistical software (TIBCO Software Inc., 2008). Log transformations were performed on SSC, streamflow, LISST concentration, and at the Clearwater River site, turbidity, to improve distribution and fit prior to the evaluation in the regression model. Various transformations were evaluated on variables prior to use in the regressions, including the square root, cube root, reciprocal root, and reciprocal, as described in Helsel and Hirsch (2002). Use of the log transformation produced the best fit and most linear relations of other evaluated transformations. Acoustic backscatter data are already reported in a log-based scale and do not require a transformation. Regression models were selected based on statistical significance (p-values) of explanatory variables and various regression statistics, such as high coefficient of determination (R^2), low standard error, constant variance and random patterns in residuals plots, and low relative percent difference (RPD) between measured and estimated SSC, as defined in equation (6):

$$\text{RPD} = [(\text{Estimated SSC} - \text{Measured SSC}) / \text{Measured SSC}] \times 100 \quad (6)$$

Additional forms of the regression models developed for the acoustic backscatter surrogates were evaluated in an attempt to improve fit at high SSC. One of the forms evaluated was a compound regression model composed of two linear segments with different slopes. A breakpoint in acoustic backscatter between the two linear segments was selected based on backscatter measured during times when upstream tributaries contributed high SSC. For example, in the Clearwater River, the evaluated breakpoint was 72 dB. Above this breakpoint, most of the samples in the Clearwater River were collected during times when high SSC was measured in the Potlatch River ([fig. 1](#)), an upstream tributary to the Clearwater River. Polynomial forms of the acoustic backscatter models also were evaluated, which included terms of backscatter and backscatter squared. None of the evaluated forms substantially improved the overall fit of the regression model to the measured data nor the variance in residuals plots, in comparison with the simple linear relations between corrected acoustic backscatter and log-transformed SSC.

A nonparametric bias correction factor described in Duan (1983) was applied to each regression model to correct for bias induced by log transformation and subsequent retransformation of the dependent variable. Duan's bias correction factor is calculated by averaging the values of 10 to the power of each residual of the dependent variable in the dataset used to develop the regression model. The factor was used to correct each value of SSC as well as upper and lower 95-percent confidence intervals estimated by a regression model. Sediment loads were calculated by multiplying estimates of SSC by rated streamflow at each study site.

Sediment-transport curves developed during the 1970s study and presented in Jones and Seitz (1980) were applied to streamflow data in the 2008–10 study to determine whether the relation between suspended sediment and streamflow changed between the two studies. Jones and Seitz (1980) did not use a bias correction factor in their equations. The original sediment-transport curves were not altered for the comparison with the 2008–10 study.

Use of Surrogate Models To Estimate Suspended Sediment

Stream conditions varied at each sediment-surrogate monitoring site. Measured SSC in the Clearwater River ranged from 3 to 210 mg/L, with a median of 13 mg/L, during the period of sample collection used for development of the surrogate models (May 2008–September 2010) ([table 1](#)). Fines content (<63 µm) ranged from 30 to 96 percent. In the Snake River, measured SSC ranged from 6 to 414 mg/L, with a median SSC of 40 mg/L. Fines content ranged

from 32 to 94 percent. Fines content at both sites typically decreased with increasing concentration. Samples were collected over nearly the full range in streamflow at both sites; 96 and 86 percent of the range in flow was represented by samples at the Clearwater River and Snake River sites, respectively ([table 1](#)).

The acoustic surrogate models demonstrate the robust nature of acoustic technologies for use as sediment surrogates at the study sites. The higher frequency acoustic surrogate models were the best estimator of SSC of all of the evaluated surrogate technologies, based on regression statistics ([tables 2](#) and [3](#)). The ADVMs also required the least maintenance of the instruments evaluated; however, post-processing of the data was more difficult than for other surrogates. Substantial variability was observed in the turbidity and laser diffraction models, which may be due in part to cross-sectional variability in sediment concentration, which was verified through the collection of the discrete samples across each cross section as well as visual observations of sediment stratification during some site visits, typically after a runoff event. At each study site, tributary inflows enter the main channel on the left bank less than 2 mi upstream of the measurement site. During some storm runoff and snowmelt events, the tributaries discharge sediment-laden water that adjoins the left bank and persists downstream past the location of the surrogate equipment. However, turbulence induced by channel and bank features varied with streamflow and seemed to cause slight spatial variability in this zone, relative to the location of the surrogate instruments. This small-scale spatial variability likely resulted in the high variability in the calibrations of the laser diffraction and turbidity instruments. The ADVMs were less affected by this streamflow condition because they sample a larger part of the channel volume and capture more of the cross-sectional variability. The method for correcting acoustic backscatter for losses assumes that the suspended sediment within the sampling volume is relatively uniform in concentration and particle-size distribution, but the acoustic surrogates seem to be more tolerant of small amounts of spatial variability than the point measurements of the laser diffraction and turbidity instruments.

Clearwater River Study Site

Backscatter from the 3-MHz ADVM was the best estimator of SSC in the Clearwater River, likely because sediment is dominated by fine sands and silt which seems to be well-targeted by the high frequency ADVM ([table 2](#)). Surrogate models also were developed to estimate sand and fines concentrations separately based on 3-MHz acoustic backscatter. RPD was calculated between each pair of measured and estimated SSC values according to equation (6).

Table 2. Surrogate model results and regression statistics for the Clearwater River at Spalding, Idaho, May 2008–September 2010.

[Sediment surrogate: ADVM, acoustic Doppler velocity meter; MHz, megahertz. Model: SSC, suspended-sediment concentration in milligrams per liter (mg/L); ABS_{corr} , acoustic backscatter corrected for beam spreading and attenuation by water and sediment in decibels (dB); Turb, turbidity in Formazin Nephelometric Units (FNU); Q , streamflow in cubic feet per second (ft^3/s); LISST, suspended-sediment concentration estimated by the LISST StreamSide in microliter per liter ($\mu\text{L/L}$). R^2 : Coefficient of determination. Average RPD: Relative percent difference. BCF: Duan's bias correction factor. Abbreviation: na, not applicable]

Sediment surrogate	Number of samples used for regression	Model	R^2	Average RPD (percent)	Standard error (mg/L)	BCF
3-MHz ADVM backscatter	30	$\text{SSC} = 10^{[(0.0557 \times 3\text{-MHz_ABScorr})^2.431]} \times 1.040$	0.93	+8.6	1.34	1.040
		Sand concentration = $10^{[(0.0743 \times 3\text{-MHz_ABScorr})^4.147]} \times 1.146$	0.87	+34	1.71	1.146
		Fines concentration = $10^{[(0.0461 \times 3\text{-MHz_ABScorr})^2.030]} \times 1.097$	0.78	+19	1.58	1.097
Turbidity	30	$\text{SSC} = 10^{[(0.872 \times \log(\text{Turb}))^{+0.454}]} \times 1.202$	0.64	+48	1.92	1.202
2008–10 sediment transport curve	33	$\text{SSC} = 10^{[(1.142 \times \log(Q))^{-3.840}]} \times 1.284$	0.54	+64	2.10	1.284
1970s sediment transport curve ¹	135	$\text{SSC} = 0.000349 \times Q^{1.074}$	0.52	+54	2.69	na ²
0.5-MHz ADVM backscatter	30	$\text{SSC} = 10^{[(0.0064 \times 0.5\text{-MHz_ABScorr})^{-0.676}]} \times 1.916$	0.007	+204	2.97	1.916
Laser diffraction	15	$\text{SSC} = 10^{[(0.0459 \times \log(\text{LISST}))^{+1.011}]} \times 1.560$	0.003	+119	2.73	1.560

¹ As published in Jones and Seitz (1980).² Bias correction factor was not used in the computation of concentrations and loads in Jones and Seitz (1980).

Table 3. Surrogate model results and regression statistics for the Snake River near Anatone, Washington, May 2008–September 2010.

Sediment surrogate: ADVM, acoustic Doppler velocity meter; MHz, megahertz. **Model:** SSC, suspended-sediment concentration in milligrams per liter (mg/L); ABS_{corr} , acoustic backscatter corrected for beam spreading and attenuation by water and sediment in decibels (dB); Turb, turbidity in Formazin nephelometric units (FNU); Q , streamflow in cubic feet per second (ft^3/s); LISST, suspended-sediment concentration estimated by the LISST StreamSide in microliter per liter ($\mu\text{L/L}$). **R**²: Coefficient of determination. **Average RPD**: Relative percent difference. **BCF**: Duran's bias correction factor. **Abbreviation:** na, not applicable

Sediment surrogate	Number of samples used for regression	Model	R ²	Average RPD (percent)	Standard error (mg/L)	BCF
1.5-MHz ADVM backscatter	22	$\text{SSC} = 10^{[(0.0756 \times 1.5\text{-MHz_ABScore}) - 4.676]} \times 1.048$	0.92	+10	1.39	1.048
		Sand concentration = $10^{[(0.105 \times 1.5\text{-MHz_ABScore}) - 7.636]} \times 1.129$	0.89	+24	1.73	1.129
		Fines concentration = $10^{[(0.0615 \times 1.5\text{-MHz_ABScore}) - 3.730]} \times 1.084$	0.81	+19	1.54	1.084
2008–10 sediment transport curve	33	$\text{SSC} = 10^{[(1.761 \times \log(Q)) - 6.697]} \times 1.120$	0.83	+24	1.65	1.120
1970s sediment transport curve ¹	125	$\text{SSC} = 0.000003 \times Q^{1.460}$	0.61	-34	2.03	na ²
Turbidity	29	$\text{SSC} = 10^{[(0.0181 \times \text{Turb}) + 1.249]} \times 1.209$	0.70	+48	1.93	1.209
0.5-MHz ADVM backscatter	22	$\text{SSC} = 10^{[(-0.0333 \times 0.5\text{-MHz_ABScore}) + 4.301]} \times 1.417$	0.33	+120	2.59	1.417

¹ As published in Jones and Seitz (1980).² Bias correction factor was not used in the computation of concentrations and loads in Jones and Seitz (1980).

The model between 0.5 MHz acoustic backscatter and SSC was poor ($R^2=0.007$) because of a problem noted in the instrument noise level measurements. At high flows, the measured noise level increased substantially and was high relative to the raw backscatter measurement. The 0.5-MHz ADVM appears to be more sensitive to electrical and other noise that occurs in the water at high streamflows than the other evaluated frequencies (Craig Huhta, SonTek/Yellow Springs Instruments, oral commun., 2012). Because the instrument noise level is subtracted from the raw backscatter to compute SNR, in many cases this resulted in a low SNR when SSC was high. For comparison, a model was developed between the raw backscatter from the 0.5-MHz ADVM (without subtracting the noise level) and SSC, resulting in an improved R^2 of 0.89, but raw backscatter data collected during this period also could have been erroneous. Overall, the 3-MHz ADVM was still a better estimator of SSC than the other surrogates whether raw backscatter or SNR was used to develop the model.

Topping and others (2004) determined that in the Colorado River, the degree of sediment attenuation along the beam path is closely related to the fines fraction, and average backscatter is closely related to the sand fraction. However, backscatter alone was determined to be a good estimator of the fines and sand fractions, as well as overall SSC, in the Clearwater River. The model between 3-MHz acoustic backscatter and SSC (overall, sand, and fines) shows that a shift from a fines-dominated SSC to a sand-dominated SSC occurs around 60 mg/L or an ABS_{corr} for the 3-MHz ADVM of 75 dB (fig. 5). Non-zero attenuation at low SSC, likely because of the presence of organic matter, created significant variability in the relation between attenuation and the fines fraction, as well as overall SSC, at low concentrations. High variability in the individual sand and fines models is caused by many physical factors of sediment load and transport including the magnitude of the washload component, mobility of bed material and armor, non-equilibrium (supply limited) transport

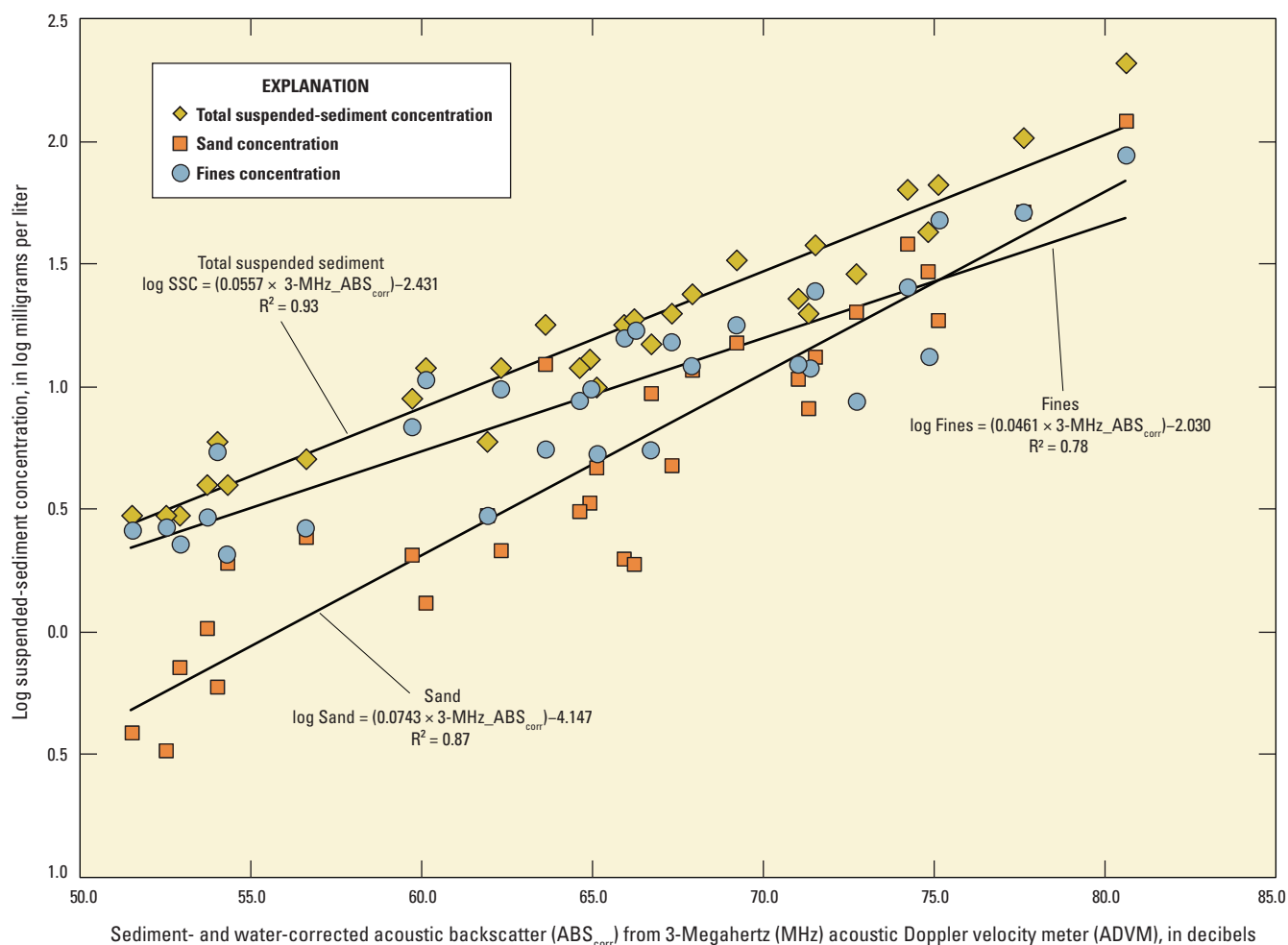


Figure 5. Surrogate regression models for total suspended sediment, sand, and fines concentrations based on acoustic backscatter for the Clearwater River near Spalding, Idaho.

of sediment, relative magnitudes of the tributary flows, timing of releases of stored water for water management, and proximity of episodic sediment sources. The uncertainty and stochasticity of the relations between these factors motivated the USACE's interest in the use of surrogate sediment measurement technology in this study.

The selected regression based on 3-MHz acoustic backscatter represented 93 percent of the variability in SSC and resulted in an average RPD between measured and estimated SSC of +8.6 percent. Standard error for the 3-MHz model was lower and variance in residuals was lower and more constant than for all other models indicating best fit. Best agreement (lowest RPD) was observed when fines were between about 70 and 85 percent of total SSC. Estimates of SSC when the sand fraction was high were not substantially improved by using the model with the 0.5-MHz ADVM, even when using a model that did not incorporate the continuously measured noise level. This is likely because most of the sand fraction is very fine and fine sand (<250 µm), which along with fines is well-represented by the 3-MHz ADVM.

Results of discrete samples collected to assess cross-sectional variability in SSC show that inflows from the upstream tributary Lapwai Creek are not well mixed with the Clearwater River at the study site under some conditions of flow. Segregation of Clearwater River and Lapwai Creek flows is supported by hydraulic analysis and observations made by aerial survey (Teasdale, 2005). Standard deviation among discrete samples ranged from 2 mg/L at low SSC to 24 mg/L at high SSC. Because water from Lapwai Creek adjoins the bank on the same side of the river as the surrogate instruments, they likely sample a zone of average to above-average SSC relative to the entire cross section. The biased sampling leads to an overestimate of sediment concentration when this phenomenon occurs. Even with this local effect, the ADVMs represent cross-sectional variability better than other surrogates. Alternative methods to correct bias imposed by non-uniform flow conditions are being evaluated.

Following a transformation back to original units, the selected regression model for estimating SSC at the Clearwater River site is:

$$\text{SSC} = 10^{[(0.0557 \times \text{3-MHz_ABS}_{\text{corr}}) - 2.431]} \times 1.040 \quad (7)$$

where

SSC is the suspended-sediment concentration (mg/L),

3-MHz_ABS_{corr} is the range-normalized acoustic backscatter from the 3-MHz ADVM corrected for two-way transmission losses (dB), and

1.040 is Duan's bias correction factor.

Measured and estimated SSC based on the selected model (eq. 7) compare well but deviate at higher SSC (>100 mg/L) ([fig. 6](#)). The upper and lower 95-percent confidence level for the sample with highest concentration, 210 mg/L, plotted well below the value estimated by the surrogate model. RPD for individual observations ranged from -43 to +80 percent, but most of the high RPDs occurred at low SSC, when small differences between estimated and measured values can result in high percent differences. At high SSC (>100 mg/L), mean RPD was -33 percent, meaning that in general, the regression model underestimated measured SSC when high. A possible reason for model underestimation at high SSC is that more sand is transported during these periods. Sand may travel lower in the water column than finer materials owing to higher mass and may not be captured within the sampling volume of the ADVMs, which are installed approximately mid-depth in the water column. An additional source of error may have been that 4 of the sample concentrations (5.1, 19, 38, and 104 mg/L) used to develop the surrogate model were averages of 10 concentrations of discrete samples collected across the cross section. However, none of these sample concentrations appear to be highly influential in the regression ([fig. 5](#)) so likely do not contribute to substantial model error. The USGS evaluated whether the inclusion of additional explanatory variables in the regression would improve estimates at high SSC. Some of the evaluated variables included the fraction

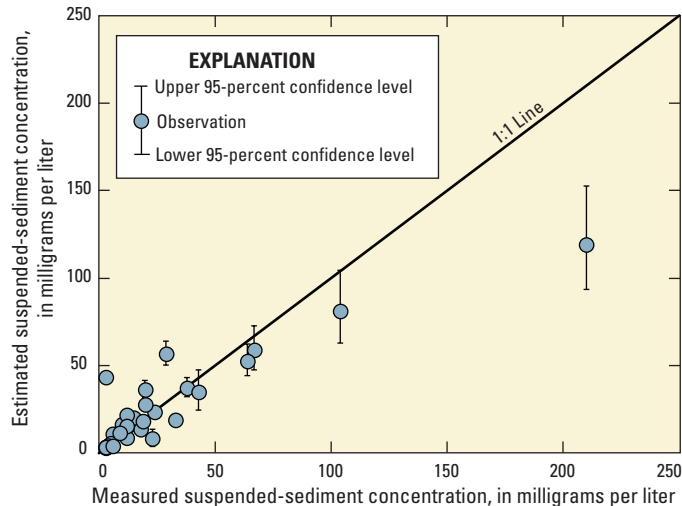


Figure 6. Measured and estimated total suspended sediment concentrations in the Clearwater River at Spalding, Idaho, based on a surrogate model with acoustic backscatter.

of unregulated flow passing the site, turbidity, the square of 3-MHz_ABS_{corr}, and ratios of attenuation and backscatter for the 3- and 0.5-MHz ADVMs. The fraction of unregulated flow term is discussed in more detail in Wood (2010). None of the variables substantially improved the regression statistics or SSC estimates in comparison with the base model using 3-MHz_ABS_{corr} alone.

At low SSC (<100 mg/L), mean RPD was +16 percent; thus the regression model generally overestimated measured SSC when low. Average percent organic matter was 10 percent at high SSC and 23 percent at low SSC. High percent organic matter at low SSC is a possible cause of high positive RPD because the ADVMs likely detect the organic matter as sediment. Inaccuracy in the estimates of the low SSC range had a negligible effect on the estimation of the magnitude

and timing of total suspended sediment load in this study, but may be of importance where chronic exposure to low levels of contaminated sediment is the concern.

Measured and estimated SSC for March–July 2010, based on the selected model with 3-MHz acoustic backscatter as well as with transport curves developed from 2008 to 2010 and 1970s samples, and streamflows, is presented in figure 7. Agreement between measured and estimated SSC is better for the 3-MHz ADVM than for the sediment-transport curves. At this site, sediment predictions based on streamflow are less accurate than those based on acoustic backscatter over a storm event. Sediment transport curves inadequately represent hysteresis of sediment concentration caused by the timing of inflows from sediment-laden tributaries and the other factors mentioned above.

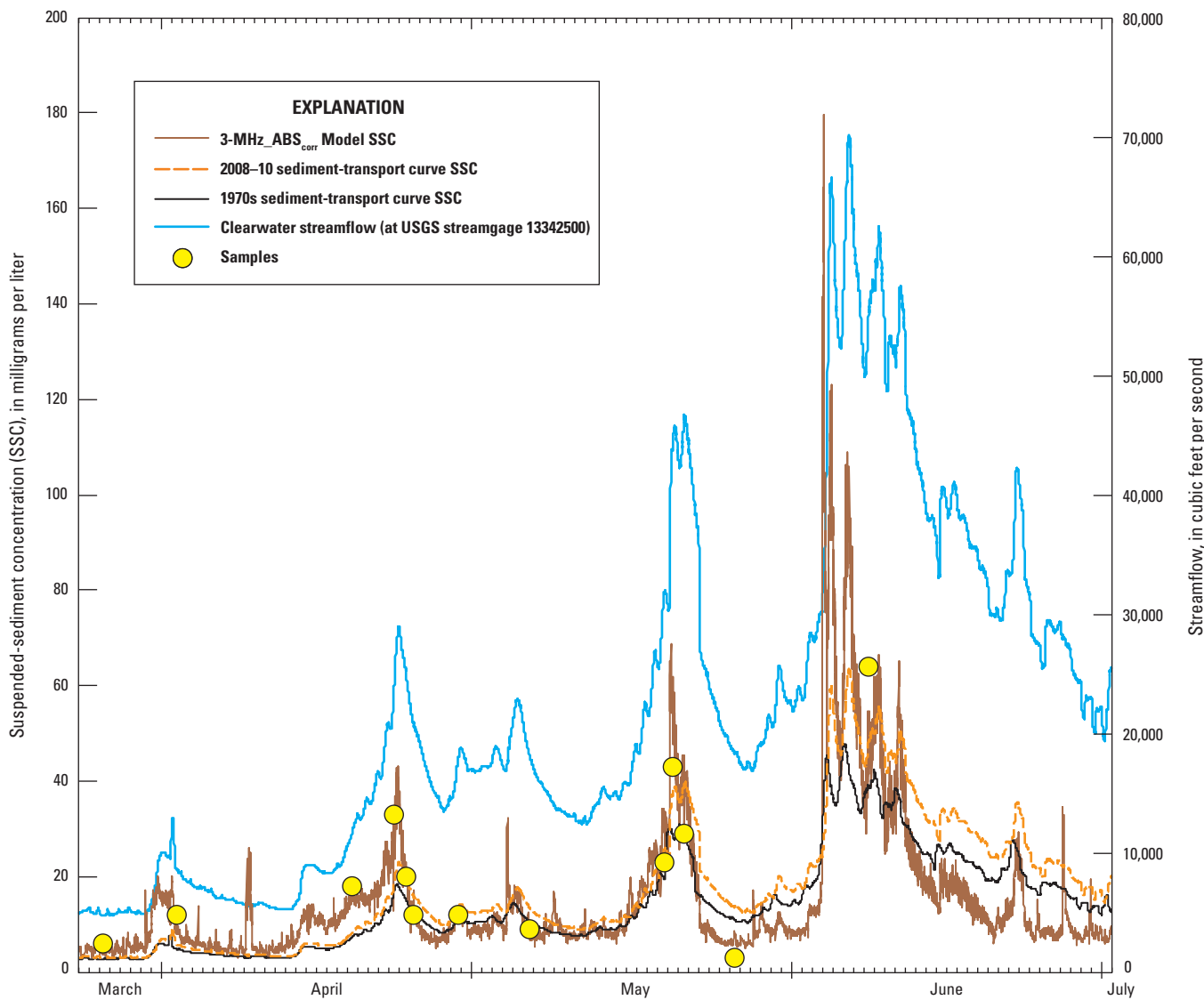


Figure 7. Estimated instantaneous values of total suspended-sediment concentration for March 23–July 1, 2010, in the Clearwater River near Spalding, Idaho, based on a surrogate model with acoustic backscatter and sediment-transport curves developed using data from the 2008–10 and 1970s studies.

Snake River Study Site

Acoustic backscatter was shown to be as good of an estimator for SSC in the Snake River as it was in the Clearwater River, despite the shorter period of record during which the ADVMs were installed and fewer samples available for the calibration ([table 3](#)). Similar to the Clearwater River, the model between 0.5-MHz ADV backscatter and SSC was poor owing to high noise levels at high flows resulting in an inverse relation between SNR and SSC. A model developed between the raw backscatter from the 0.5-MHz ADV (without subtracting the noise level) and SSC resulted in an improved R^2 of 0.67 but was still inferior to the model between the 1.5-MHz ADV and SSC.

Discrete samples collected to assess cross-sectional variability in SSC show that inflows from the upstream tributary Grande Ronde River are not always well-mixed with the Snake River at the study site. Standard deviation among discrete samples was higher for the Snake River than for the Clearwater River, ranging from 15 mg/L at low SSC to 185 mg/L at high SSC. The surrogate instruments likely measure a zone of average to above-average SSC relative to the entire cross section because water from the Grande

Ronde River adjoins the left bank and does not fully mix with the Snake River flow before the measurement site. As at the Clearwater River site, the ADVMs at the Snake River site are able to better represent cross-sectional variability than other surrogates.

Following a transformation back to original units, the selected regression model for estimating SSC at the Snake River site is:

$$\text{SSC} = 10^{[(0.0756 \times 1.5\text{-MHz_ABS}_{\text{corr}}) - 4.676]} \times 1.048 \quad (8)$$

where

SSC is the suspended-sediment concentration (mg/L),

$1.5\text{-MHz_ABS}_{\text{corr}}$ is the range-normalized acoustic backscatter from the 1.5-MHz ADVM corrected for two-way transmission losses (dB), and

1.048 is Duan's bias correction factor.

Separate models were developed to estimate overall SSC as well as sand and fines fractions ([fig. 8](#)). The shift from a fines-dominated SSC to a sand-dominated SSC appears to occur at about 110 mg/L or an ABS_{corr} for the 1.5-MHz ADVM of 89 dB.

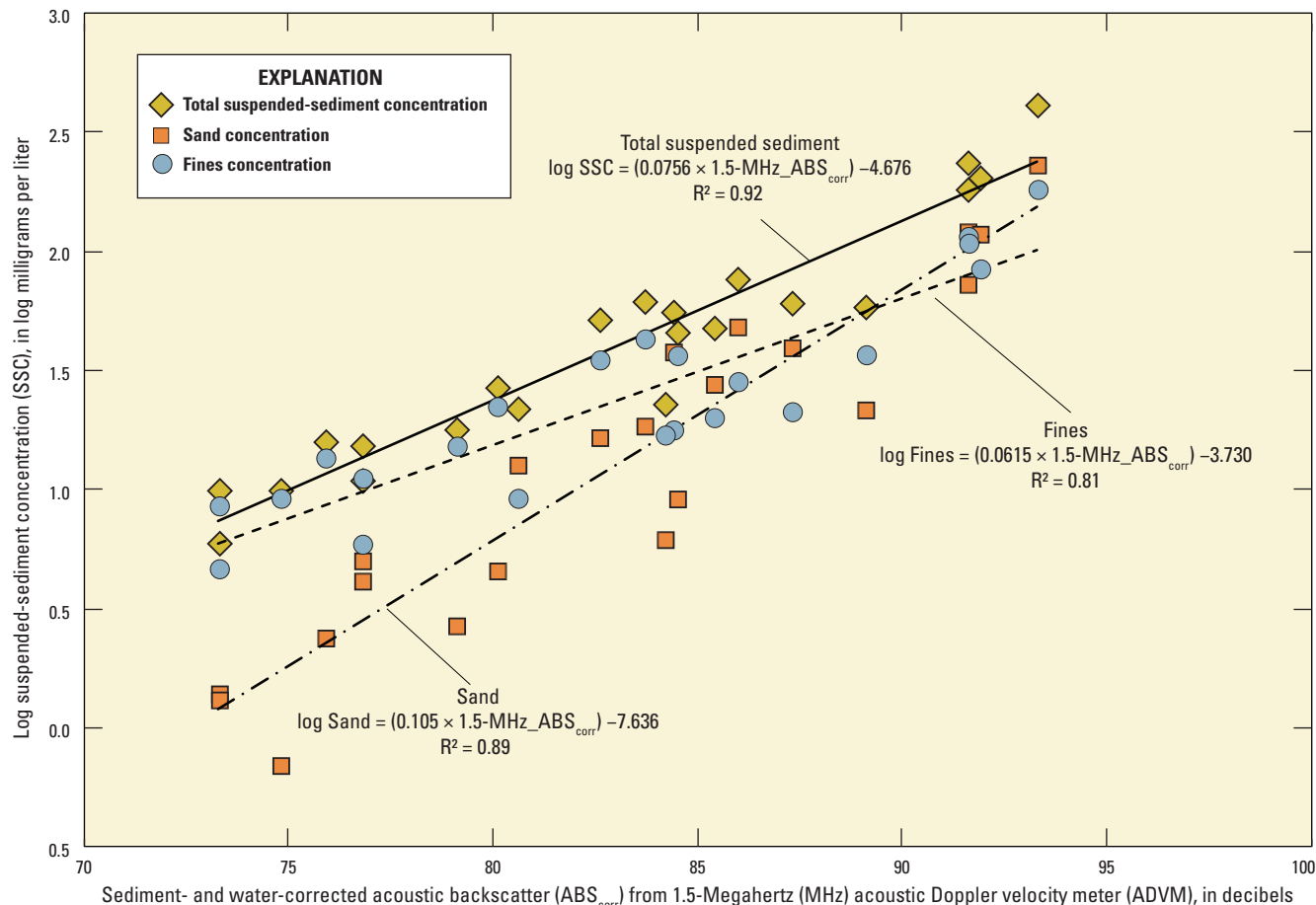


Figure 8. Surrogate regression models for total suspended sediment, sand, and fines concentrations based on acoustic backscatter for the Snake River near Anatone, Washington.

In general, agreement between measured and estimated SSC improved as the percentage of fines increased. Similar to the Clearwater River, estimates of SSC when the sand fraction was high were not significantly improved by using the model with the 0.5-MHz ADVM, even when using a model that did not incorporate the continuously measured noise level. Based on a grain-size analysis of the full sand fraction conducted for 12 of the samples, most of the sand fraction appears to be very fine and fine sand (<250 μm) with some medium sand (<500 μm), which along with fines appears to be fairly well-represented by the 1.5-MHz ADVM.

Measured and estimated SSC based on the selected model (eq. 8) shows good agreement but some deviation at high SSC (fig. 9). RPD for individual observations ranged from -40 to +123 percent, but many of the high RPDs were at low SSC, when small differences between the estimated and measured values can result in high percent differences. At high SSC (>100 mg/L), mean RPD was -16 percent, meaning that in general, the regression model underestimated true SSC when high. Similar to the Clearwater River, model underestimation at high SSC likely occurs because more sand is transported during these periods, which may travel lower in the water column than finer materials owing to higher

mass and may not be captured within the sampling volume of the ADVMs. Estimates at high SSC may be improved by collecting samples to define the degree of vertical stratification of sediment and by installing another ADVM at a depth likely to capture the zone of sand transport. Similar to the Clearwater River analysis, the USGS evaluated whether the inclusion of additional explanatory variables in the regression would improve estimates at high SSC. Some of the evaluated variables included fraction of unregulated flow passing the site (discussed in Wood (2010) for a preliminary analysis of the Snake River data), turbidity, the square of 1.5-MHz_ABS_{corr}, and ratios of attenuation and backscatter for the 1.5- and 0.5-MHz ADVMs. In the final analysis, none of the variables substantially improved the regression statistics or SSC estimates in comparison with the base model using 1.5-MHz_ABS_{corr} alone.

At low SSC (<100 mg/L), mean RPD was +16 percent; thus, the regression model generally overestimated true SSC when low. Similar to the Clearwater River site, percent organic matter at low SSC was higher (16 percent) than at high SSC (5 percent) and is a possible cause of high positive RPD in those samples. Overall, however, measured and estimated SSC compared well, matching on average within 10 percent.

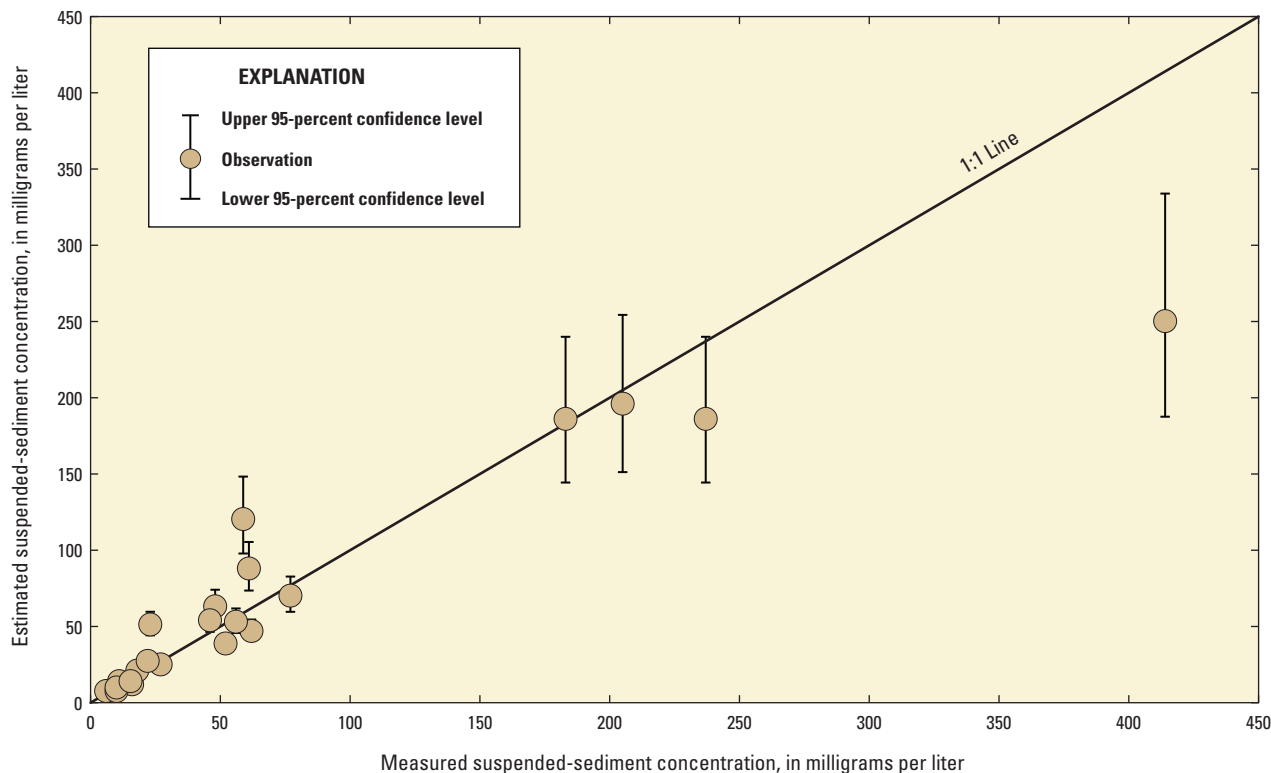


Figure 9. Measured and estimated total suspended-sediment concentrations in the Snake River near Anatone, Washington, based on a surrogate model with acoustic backscatter.

Measured and estimated SSC, based on the selected regression model as well as sediment-transport curves based on 2008–10 and 1970s samples and streamflows, are shown for a selected high flow event in June 2010 in figure 10. The highest SSC sample collected during the period of analysis (414 mg/L) was collected during this event but was not well-represented by any of the surrogate models. The peak in sediment concentration estimated by the acoustic backscatter model on June 3 on the ascending limb of the hydrograph was caused by an increase in sediment-laden inflows from the Salmon River. Because the increase in Salmon River flow was proportional to the increase in total flow at the study site, but sediment contributions were not, the increase in sediment concentrations estimated at the study site was not well-represented by the sediment-transport curves.

As a whole, the concentrations and loads calculated using the 1970s sediment-transport curve underestimate current sediment transport. If the estimates based on acoustic backscatter are assumed to be more accurate, then estimates using the 2008–10 sediment-transport curve underestimate sediment transport on the ascending limb and peak of the hydrograph and overestimate current sediment transport on the descending limb of the hydrograph. The differences between sediment loads estimated using sediment transport curves developed from 2008–10 and 1970s streamflows were much greater for the Snake River than the Clearwater River. Based on other sampling conducted by the USGS in the Snake River basin, the Salmon River transported more sediment (particularly sand) in the 2008–10 study than in the 1970s study (Clark and others, 2013).

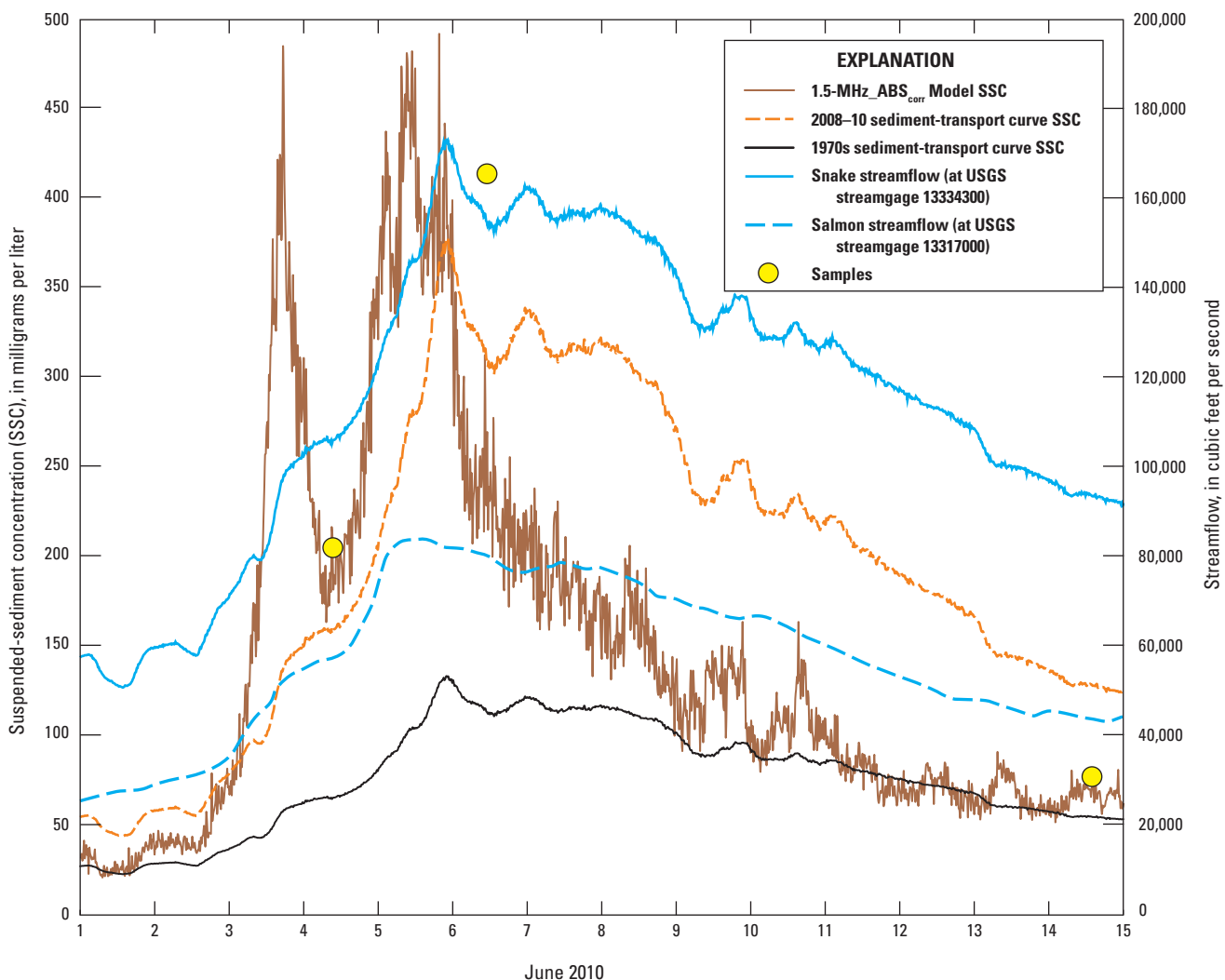


Figure 10. Estimated instantaneous values of suspended-sediment concentration during a storm event on June 1–15, 2010, in the Snake River near Anatone, Washington, based on a surrogate model with acoustic backscatter and sediment transport curves developed using data from the 2008–10 and 1970s studies.

Advantages of Acoustics over Sediment-Transport Curves in Sediment Monitoring

Use of regression models that relate measured SSC to streamflow is common practice in sedimentation engineering (Glysson, 1987; Gray and Simões, 2008) and is often necessary when sediment load must be predicted for forecast or hypothetical streamflows. In sediment load monitoring, SSC is often estimated on a continuous basis using a sediment-transport curve or linear regression, but such relations are often not accurate over short time scales because the regression prediction is for the mean SSC response. This is particularly true when estimating SSC for a particular storm event where sediment supply is the limiting factor of sediment transport and is not well represented by the mean response.

These inaccuracies arise in simple univariate regression because the same SSC is predicted at identical streamflows on the ascending and descending limbs of the hydrograph, although the actual sediment load may be strongly hysteretic. In addition, streamflows in rivers that are partially regulated may be comprised of relatively non-turbid water management releases, sediment-laden tributary inflows and overland runoff. Under these conditions, the dominant sediment sources may not contribute a large percentage of flow but contribute most of the sediment load. It follows that a large increase in flow owing to a regulated flow release may not equate to a corresponding increase in SSC. Furthermore, sudden increases in SSC because of increased sediment transport from unregulated tributaries will not be represented by a simple streamflow-sediment load regression derived for the main river unless such events were adequately represented in the regression dataset.

More complex approaches may be used to estimate composite load with separate regressions for each source, a multivariate relation (Helsel and Hirsch, 2002), or a model simulation. Load monitoring with ADVMs provides a more direct means to improve the accuracy of continuous sediment-load estimates.

The effect of tributary sediment inflow is seen in [figure 7](#) which shows an increase in SSC estimated by acoustic backscatter in the Clearwater River on April 8, 2010, because of a storm event in the Lapwai River drainage that was not estimated by the 2008–10 or 1970s sediment-transport curves. In the Snake River in June 2010 ([fig. 10](#)), assuming that acoustic backscatter was the most accurate estimator of SSC, a small increase in flow on the ascending limb of the hydrograph owing to increases in flow from the Salmon River caused a large increase in estimated SSC that was not captured in 2008–10 and 1970s sediment-transport curve estimates.

The timing of sediment sample collection also has been traditionally targeted for capturing the peak of the hydrograph, which may or may not coincide with peak SSC. At the study sites, SSC estimated by the acoustic backscatter surrogate models typically peaks on the ascending limb of the hydrograph then decreases fairly rapidly after peak streamflow ([figs. 7](#) and [10](#)). It is rational that higher concentrations would be observed on the ascending limb owing to a “first flush” effect from overland runoff, tributary inflows, and resuspension of sediment from the stream channel. A surrogate model other than streamflow is needed to help guide sediment sampling efforts as well as to capture the variability in SSC during an event.

Comparison over Short Time Scales

To further quantify differences in suspended-sediment concentration and load estimates over short time scales, suspended-sediment loads were summed by month and for the duration of selected, well-defined hydrologic events. The range and distribution of SSC in the Clearwater River, analyzed by month during the period of analysis based on 3-MHz acoustic backscatter, shows several outliers with high SSC because the 3-MHz surrogate model tends to capture short-term increases in SSC ([fig. 11A](#)). Most storm and rain-on-snow events occur in April and May (including June 2010), and streamflow begins to decline in later June and July. Except for outliers, the estimated range and overall distribution in SSC is higher for the 2008–10 sediment-transport curves than for the acoustic backscatter models during the high flow months (April, May, June) and for months with declining flows (July, August) ([fig. 11B](#)). This pattern indicates that the 2008–10 sediment-transport curve does not represent conditions during individual storm events owing to hysteresis but, on a monthly basis, the transport curve overestimation of sediment on the descending limb of the hydrograph results in an overall net concentration that is higher than what is estimated using the acoustic backscatter model. Monthly SSC estimated by the 1970s sediment-transport curves were similar in pattern but slightly lower in magnitude compared with the 2008–10 sediment-transport curves. The 3-MHz surrogate model and 1970s and 2008–10 sediment-transport curves estimate similar concentrations during September through March when flows are fairly steady and storm events are infrequent. Monthly SSCs in the Snake River are similar in pattern but higher in magnitude compared to those in the Clearwater River.

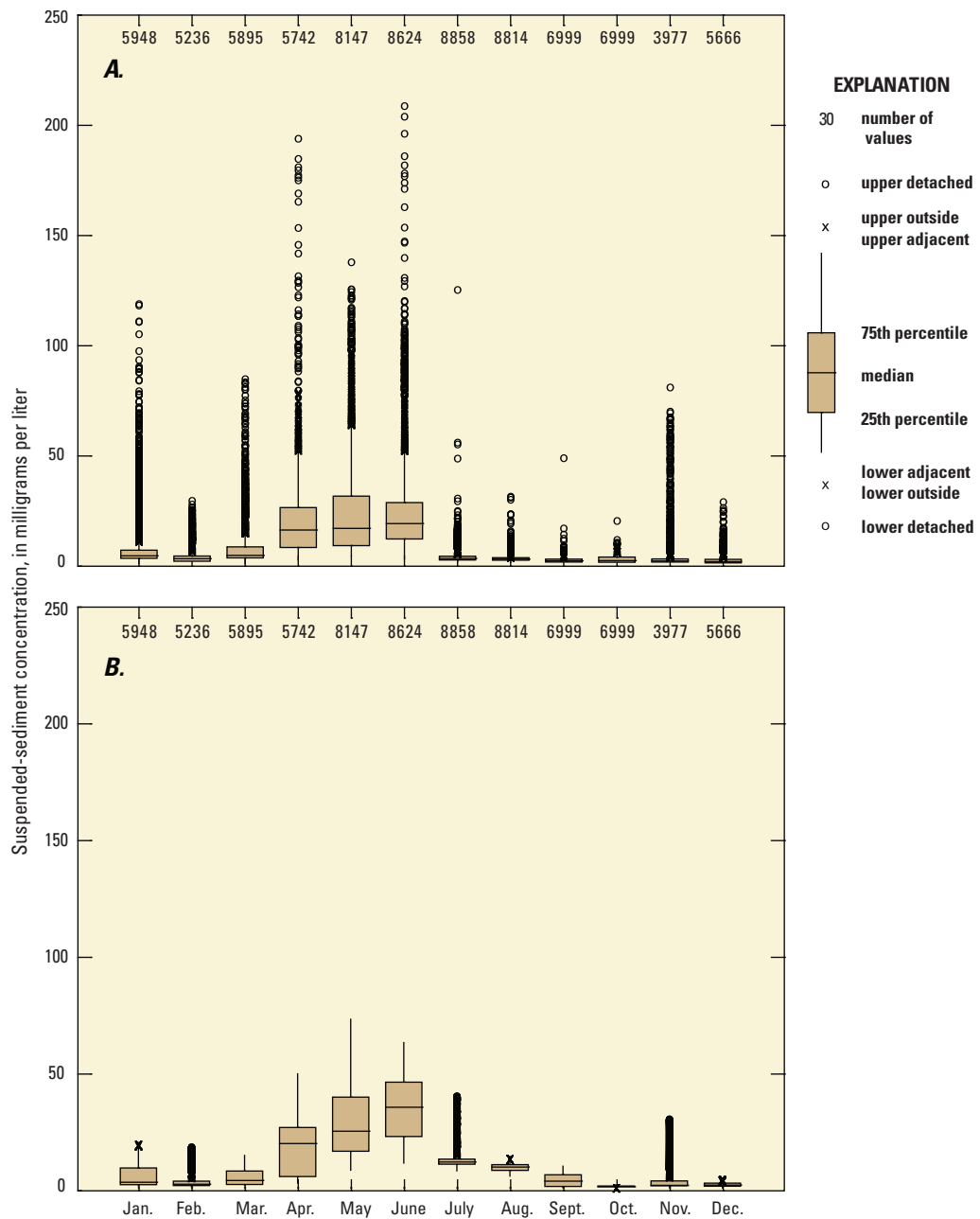


Figure 11. Distribution of total suspended-sediment concentration by month in the Clearwater River at Spalding, Idaho, based on (A) a surrogate model with 3MHz acoustic backscatter, (B) 2008–10 sediment transport curves, and (C) 1970s sediment transport curves, May 2008–September 2010.

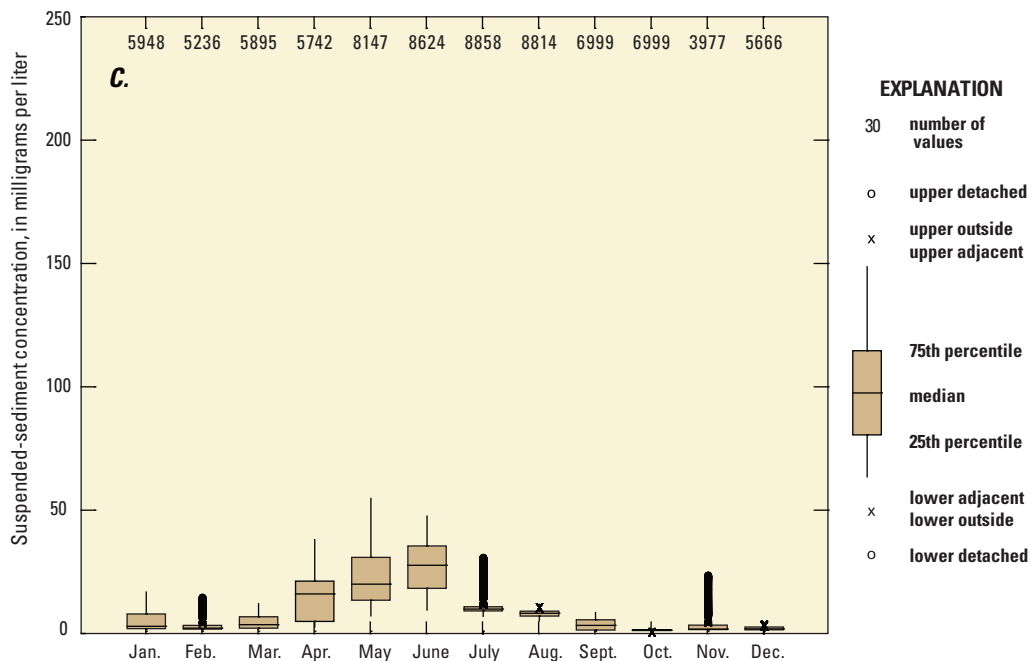


Figure 11.—Continued

Monthly patterns also are evident in figure 12, which presents total load by month for both study sites for the acoustic backscatter model and 1970s and 2008–10 sediment-transport curves. At the Clearwater River study site (fig. 12A), the 1970s sediment-transport curves estimate lower sediment loads during months when flow generally is increasing (April–May) and higher monthly sediment loads during months when flow is high or generally decreasing (June–August) relative to the acoustic backscatter model. At the Snake River study site, estimates generated from the 1970s sediment-transport curves are much lower than those generated from the acoustic backscatter model and 2008–10 sediment-transport curve during April–June and similar to those generated from the acoustic backscatter model during other months.

Differences in load estimates owing to hysteresis were further examined by summing estimated loads over the ascending and descending limbs of the hydrograph for several well-defined hydrologic events—seven in the Clearwater River and six in the Snake River (table 4). Load estimates based on acoustic backscatter were higher on the ascending limb (negative percent difference) and lower on the

descending limb (positive percent difference) than estimates based on the 2008–10 sediment-transport curves in all cases except the descending limb for two events in the Clearwater River. Loads for these two events were low relative to other events. For all events combined, load estimates based on acoustic backscatter were 15 and 35 percent higher on the ascending limb and 30 and 49 percent lower on the descending limb than estimates based on 2008–10 sediment-transport curves for the Clearwater and Snake Rivers, respectively. Estimated SSC was usually higher on the ascending limb (especially for acoustic backscatter) but total loads were often higher on the descending limb because of a prolonged recession in flow. Loads estimated by the 1970s sediment-transport curves were not included in the storm event analysis because patterns are expected to be similar to the 2008–10 sediment-transport curves. In this study, acoustic backscatter appears to be a better estimator of sediment for load monitoring than streamflow alone over short time scales because it (1) is not affected by hysteresis, (2) provides a more direct, in-situ measurement of suspended sediment, and (3) better represents sediment sources from a combination of regulated and unregulated sources.

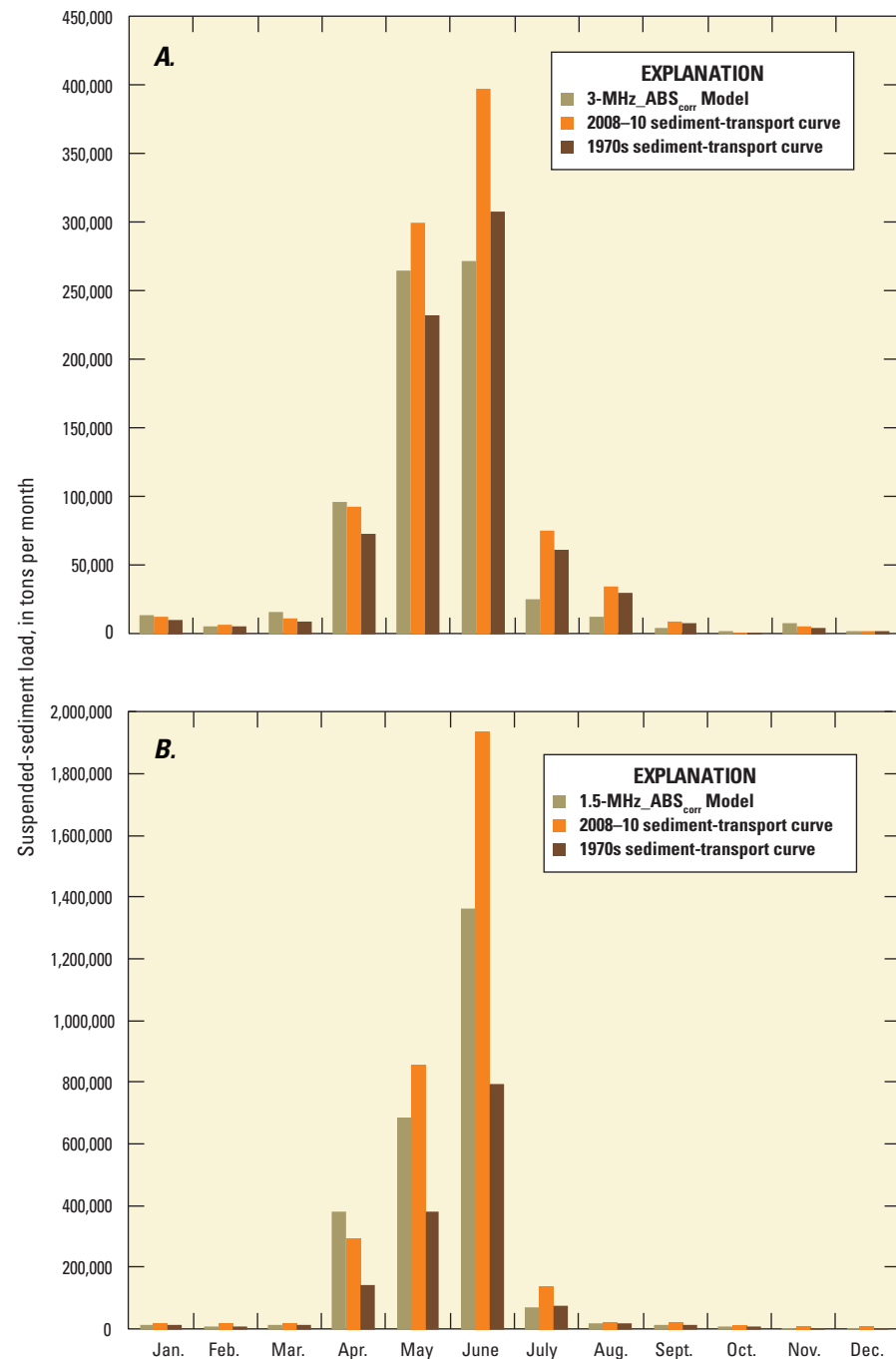


Figure 12. Total suspended-sediment load by month based on a surrogate model with acoustic backscatter and 2008–10 and 1970s sediment-transport curves for the (A) Clearwater River at Spalding, Idaho, May 2008–September 2010, and (B) Snake River near Anatone, Washington, April 2009–September 2010.

NOTE: Each month represents the total load that occurred during that month within the study period. For example, the total load for May in the Clearwater River is the sum of loads measured in May 2008, May 2009, and May 2010.

Table 4. Comparison of suspended sediment loads during selected storm events estimated using acoustic backscatter and sediment-transport curves based on 2008–10 streamflows in the Clearwater River at Spalding, Idaho, and Snake River near Anatone, Washington.

[Abbreviations: ABS_{corr} acoustic backscatter corrected for beam spreading and attenuation by water and sediment in decibels (dB); na, not applicable]

Site	Event No.	Event dates	Sediment load for ascending limb of hydrograph (tons)			Sediment load for descending limb of hydrograph (tons)		
			3-MHz_ABS _{corr} or 1.5-MHz_ABS _{corr} model		2008–10 sediment transport curve	Percent difference	3-MHz_ABS _{corr} or 1.5-MHz_ABS _{corr} model	2008–10 sediment transport curve
			3-MHz_ABS _{corr}	1.5-MHz_ABS _{corr}				
Clearwater River	na	na – All 7 events combined	172,000	148,000	-15	131,000	178,000	30
	1	May 13–24, 2008	59,400	56,700	-5	13,000	18,800	36
	2	November 12–30, 2008	2,070	1,120	-60	3,750	2,850	-27
	3	January 1–12, 2009	2,950	790	-116	3,540	2,700	-27
	4	April 21–May 1, 2009	13,000	12,900	-1	17,700	24,600	33
	5	May 18–June 12, 2009	9,130	8,170	-11	51,100	62,600	20
	6	May 14–26, 2010	14,700	11,200	-27	7,370	10,200	32
	7	June 2–July 5, 2010	70,600	57,200	-21	34,900	56,000	46
Snake River	na	na – All 6 events combined	585,000	409,000	-35	762,000	1,260,000	49
	1	April 18–May 3, 2009	122,000	68,500	-56	89,600	113,000	23
	2	May 5–11, 2009	48,600	39,400	-21	24,400	31,200	24
	3	May 18–24, 2009	98,400	84,100	-16	106,000	129,000	20
	4	April 20–27, 2010	15,700	11,300	-33	12,100	15,300	23
	5	May 16–30, 2010	33,000	26,600	-21	48,400	73,000	41
	6	June 2–19, 2010	267,000	180,000	-39	481,000	895,000	60

Comparison over Annual Time Scales

Total sediment loads were computed for the period of analysis using continuous estimates of SSC based on models with acoustic backscatter and sediment-transport curves based on 2008–10 and 1970s streamflows to determine how estimates compared over longer time scales ([table 5](#)). The period of analysis for each site was limited to the period when the ADVMs were deployed so that a direct comparison could be made between sediment-transport curves and acoustic surrogate models. On an annual basis, the 2008–10 sediment-transport curves produced load estimates that were +27 and +26 percent different for the Clearwater and Snake Rivers, respectively, from load estimates based on acoustic backscatter, meaning that the sediment-transport curves estimated more sediment than acoustic backscatter. Annual load estimates for the Clearwater River based on the 1970s transport curves were about 24 percent lower than estimates based on the 2008–10 sediment-transport curves; thus for a given flow, slightly more sediment was transported in the 2008–10 study than in the 1970s study. In the Snake

River, load estimates based on the 1970s transport curves were 77 percent lower than estimates based on the 2008–10 transport curves and 54 percent lower than estimates based on acoustic backscatter. For a given streamflow, much more sediment was transported in the 2008–10 study than in the 1970s study.

Overall, the acoustic backscatter model appears to be more accurate than sediment-transport curves over an annual time scale because of the patterns observed over shorter time scales (monthly and storm events). Based on the few samples collected on the receding limbs of storm hydrographs and during the long recession in flow from July to September, the sediment-transport curves overestimate sediment concentrations and loads during these flow conditions. As a result, computed annual suspended sediment is consistently higher for the sediment-transport curves than for the acoustic backscatter models.

Table 5. Comparison of total, daily, and annual suspended sediment loads estimated using acoustic backscatter and sediment-transport curves based on 2008–10 and 1970s streamflows in the Clearwater River at Spalding, Idaho, and Snake River near Anatone, Washington.

[**Sediment surrogate:** ADVM, acoustic Doppler velocity meter; MHz, megahertz. **Abbreviations:** ton/d, ton per day; ton/yr, ton per year]

Site	Sediment surrogate	Period of analysis	Total sediment load (tons)	Average daily load (ton/d)	Average annual load (ton/yr)	Percent difference in average annual load between acoustic surrogate model and sediment transport curves (percent)
Clearwater River	3-MHz ADVM backscatter	May 8, 2008–September 30, 2010	721,000	824	300,400	
	2008–10 sediment transport curve		944,000	1,079	394,000	27
	1970s sediment transport curve		742,000	848	309,000	3
Snake River	1.5-MHz ADVM backscatter	April 2, 2009–September 30, 2010	2,580,000	4,720	1,720,000	
	2008–10 sediment transport curve		3,350,000	6,120	2,230,000	26
	1970s sediment transport curve		1,480,000	2,700	987,000	-54

Summary and Conclusions

The U.S. Geological Survey, in cooperation with the U.S. Army Corps of Engineers, evaluated the use of acoustic backscatter, turbidity, laser diffraction, and streamflow as surrogate technologies to estimate real-time suspended-sediment concentrations (SSC) and loads in the Clearwater and Snake Rivers during 2008–10. Acoustic backscatter, measured using acoustic Doppler velocity meters (ADVMs), had the best relation with measured SSC, was less affected by biological fouling, and could be measured in a larger part of the channel than the other evaluated surrogate technologies. As a result, ADVMs capture more of the cross-sectional variability that is represented in the physical sediment samples collected at the study sites. Although organic matter concentrations were low at both sites, they most likely contributed to model error at low SSC. Model error at high SSC may have been partially due to vertical stratification of sediment (particularly sand), which was not always well-represented in the fixed-depth, horizontal sampling volume of the ADVMs. Improved estimates of SSC when sand concentrations are high may be obtained by installing an ADVM lower in the water column to measure backscatter in zones where sand is likely transported.

Overall, a single frequency ADVM was adequate to estimate suspended sediment in most of the streamflow conditions at both study sites, and optimal frequency was dependent on sediment characteristics. Acoustic backscatter provides improved estimates of suspended sediment concentration and load over traditional sediment-transport curves based on streamflow over short (monthly and storm event) and long (annual) time scales when sediment load is highly variable. In addition, acoustic backscatter better represents sediment contributions from a combination of regulated and unregulated sources, which can be difficult to represent with a univariate sediment-transport curve.

Sediment-surrogate technologies can be a cost-effective component of a long-term fluvial sediment monitoring program. Once an initial regression model is developed between surrogate data and SSC, samples can be collected less frequently, thus reducing long-term operation and maintenance costs for a sediment monitoring station. Sediment surrogates also allow the estimation of sediment when it is unsafe to sample the stream, such as during flood events. Inspection of the sediment record, estimated using a surrogate model, may reveal significant episodic sediment-transport events that would be difficult to detect otherwise. Traditional suspended-sediment estimation techniques using streamflow

alone may provide poor results over small time scales or in streams with partially regulated flow, episodic sediment sources, and non-equilibrium sediment transport, as is the case for the Clearwater and Snake Rivers. Sediment-surrogate technologies are an effective means to obtain continuous, accurate estimates of suspended sediment concentrations and loads for general monitoring and sediment-transport modeling. In the Clearwater and Snake Rivers, estimates of SSC using surrogate models will allow water managers and scientists to identify the timing, magnitude, and duration of high sediment load and to better monitor long-term basin response to sediment-management strategies.

Acknowledgments

The authors wish to thank USGS employees Joseph Bunt (retired), Peter Elliott, Justin Schultz, and Doug Ott for their assistance in establishing and operating the sediment surrogate instruments. Special thanks go to hydrologists and hydrologic technicians from the USGS Idaho Water Science Center's Boise and Post Falls Field Offices for assistance with sediment and streamflow data collection. The authors are grateful to fellow members of the USGS Sediment Acoustics Leadership Team for advancing and guiding the development of sediment surrogate techniques and providing valuable advice throughout the study.

References Cited

- Agrawal, Y.C., Whitmire, Amanda, Mikkelsen, Ole A., and Pottsmith, H.C., 2008, Light scattering by random shaped particles and consequences on measuring suspended sediments by laser diffraction: *Journal of Geophysical Research*, v. 113, 11 p.
- Chanson, H., Takeuchi, M., and Trevethan, M., 2008, Using turbidity and acoustic backscatter intensity as surrogate measures of suspended sediment concentration in a small subtropical estuary: *Journal of Environmental Management*, v. 88, 11 p.
- Clark, G.M., Fosness, R.L., and Wood, M.S., 2013, Sediment transport in the lower Snake and Clearwater River basins, Idaho and Washington, 2008–2011. U.S. Geological Survey Scientific Investigations Report 2013-5083, 56 p. (Also available at <http://pubs.usgs.gov/sir/2013/5083/>.)

- Deines, K.L., 1999, Backscatter estimation using broadband acoustic Doppler current profilers, in IEEE Sixth Working Conference on Current Measurement, March 11–13, 1999: San Diego, Calif., [Proceedings], p. 249–253.
- Downing, A., Thorne, P.D., and Vincent, C.E., 1995, Backscattering from a suspension in the near field of a piston transducer: Journal of the Acoustical Society of America, v. 97, no. 3, p. 1614–1620.
- Duan, N., 1983, Smearing estimate—A nonparametric retransformation method: Journal of the American Statistical Association, v. 78, p. 605–610.
- Elci, S., Aydln, R., and Work, P.A., 2009, Estimation of suspended sediment concentration in rivers using acoustic methods: Environmental Monitoring and Assessment, v. 159, no. 1–4, p. 255–265.
- Flammer, G.H., 1962, Ultrasonic measurement of suspended sediment: U.S. Geological Survey Bulletin 1141-A, 48 p.
- Gartner, J.W., 2004, Estimating suspended solids concentrations from backscatter intensity measured by acoustic Doppler current profiler in San Francisco Bay, California: Marine Geology, v. 211, p. 169–187.
- Gartner, J.W., and Gray, J.R., 2005, Summary of suspended-sediment technologies considered at the Interagency Workshop of Turbidity and Other Sediment Surrogates—Proceedings of the Federal Interagency Sediment Monitoring Instrument and Analysis Research Workshop, September 9–11, 2003, Flagstaff, Arizona: U.S. Geological Survey Circular 1276, p. 1–15.
- Glysson, G.D., 1987, Sediment-transport curves: U.S. Geological Survey Open-File Report 87–218, 47 p. (Also available at <http://pubs.er.usgs.gov/publication/ofr87218>.)
- Gray, J.R., and Gartner, J.W., 2010, Surrogate technologies for monitoring suspended-sediment transport in rivers, in Poleto, Cristiano, and Charlesworth, Susanne, eds., Sedimentology of Aqueous Systems: Wiley-Blackwell, London, chap. 1, p. 3–45.
- Gray, J.R., and Simões, F.J.M., 2008, Estimating sediment discharge, in Garcia, M.H., ed., Sedimentation engineering—processes, measurements, modeling, and practice: American Society of Civil Engineers, Manual 110, p. 1,067–1088.
- Helsel, D.R., and Hirsch, R.M., 2002, Statistical methods in water resources: U.S. Geological Survey Techniques of Water-Resources Investigations, book 4, chap. A3, 522 p. (Also available at http://pubs.usgs.gov/twri/twri4a3.)
- Jones, M.L., and Seitz, H.R., 1980, Sediment transport in the Snake and Clearwater Rivers in the vicinity of Lewiston, Idaho: U.S. Geological Survey Open-File Report 80–690, 179 p. (Also available at <http://pubs.er.usgs.gov/publication/ofr80690>.)
- Lietz, A.C., and Debiak, E.A., 2005, Development of rating curve estimators for suspended-sediment concentration and transport in the C-51 canal based on surrogate technology, Palm Beach County, Florida, 2004–05: U.S. Geological Survey Open-File Report 2005–1394, 25 p. (Also available at <http://pubs.usgs.gov/of/2005/1394>.)
- Meral, R., 2008, Laboratory evaluation of acoustic backscatter and LISST methods for measurements of suspended sediments: Sensors, v. 8, no. 2, 16 p.
- Nolan, K.M., Gray, J.R., and Glysson, G.D., 2005, Introduction to suspended-sediment sampling: U.S. Geological Survey Scientific Investigations Report 2005–5077, CD-ROM. (Also available at <http://pubs.usgs.gov/sir/2005/5077>.)
- Patino, Eduardo, and Byrne, M.J., 2004, Application of acoustic and optic methods for estimating suspended-solids concentrations in the St. Lucie River Estuary, Florida: U.S. Geological Survey Scientific Investigations Report 2004–5028, 23 p. (Also available at <http://pubs.usgs.gov/sir/2004/5028>.)
- Porterfield, G., 1972, Computation of fluvial-sediment discharge: U.S. Geological Survey Techniques of Water-Resources Investigations, book 3, chap. C3, 66 p. (Also available at <http://pubs.usgs.gov/twri/twri3-c3>.)
- Rasmussen, T.J., Ziegler, A.C., and Rasmussen, P.P., 2005, Estimation of constituent concentrations, densities, loads, and yields on lower Kansas River, northeast Kansas, using regression models and continuous water-quality modeling, January 2000 through December 2003: U.S. Geological Survey Scientific Investigations Report 2005–5165, 117 p. (Also available at <http://pubs.usgs.gov/sir/2005/5165>.)
- Reichel, G., and Nachtnebel, H.P., 1994, Suspended sediment monitoring in a fluvial environment: advantages and limitations applying an acoustic Doppler current profiler: Water Research, v. 28, no. 4, p. 751–761.
- Runkel, R.L., Crawford, C.G., and Cohn, T.A., 2004, Load Estimator (LOADEST)—A FORTRAN program for estimating constituent loads in streams and rivers: U.S. Geological Survey Techniques and Methods, book 4, chap. A5, 69 p.
- Schulkin, M., and Marsh, H.W., 1962, Sound absorption in sea water: Journal of the Acoustical Society of America, v. 34, no. 6, p. 864–865.

- SonTek/Yellow Springs Instruments, 2007, Argonaut-SL system manual firmware version 11.8: San Diego, Calif., SonTek/YSI Inc., 314 p.
- Teasdale, G.N., 2005, Satellite and aerial imaging in characterization, hydrologic analysis and modeling of inland watersheds and streams: Pullman, Wash., Washington State University, Department of Civil and Environmental Engineering, Ph.D. dissertation.
- Teasdale, G.N., 2010, Sediment load, transport and accumulation in Lower Granite Reservoir on the Snake River—Proceedings of the 2nd Joint Federal Interagency Conference, Las Vegas, Nevada, June 27–July 1, 2010: Reston, Virginia, Advisory Committee on Water Information.
- Thevenot, M.M., and Kraus, N.C., 1993, Comparison of acoustical and optical measurements of suspended material in the Chesapeake Estuary: *Journal of Marine Environmental Engineering*, v. 1, p. 65–79.
- TIBCO Software Inc.[®], 2008, TIBCO Spotfire S-+ 8.1 function guide, 148 p., accessed October 26, 2012, at www.msi.co.jp/splus/support/download/V81/functionguide.pdf.
- Topping, D., Melis, T., Rubin, D., and Wright, S.A., 2004, High-resolution monitoring of suspended-sediment concentration and grain size in the Colorado River using laser-diffraction instruments and a three-frequency acoustic system, in Liu, Cheng, ed., *Proceedings of the 9th International Symposium on River Sedimentation*, October 18–21, 2004, Yichang, China: Tsinghua University Press, Beijing, China, p. 2,507–2,514.
- Topping, D., Wright, S.A., Melis, T.S., and Rubin, D.M., 2006, High-resolution monitoring of suspended-sediment concentration and grain size in the Colorado River using laser-diffraction instruments and a three-frequency acoustic system—*Proceedings of the 8th Federal Interagency Sedimentation Conference*, April 2–6, 2006, Reno, Nevada: CD-ROM, ISBN 0-9779007-1-1, p. 539–546.
- Uhrich, M.A., and Bragg, H.M., 2003, Monitoring instream turbidity to estimate continuous suspended-sediment loads and yields and clay-water volumes in the Upper North Santiam River Basin, Oregon, 1998–2000: U.S. Geological Survey Water-Resources Investigations Report 03-4098, 44 p. (Also available at <http://pubs.er.usgs.gov/publication/wri034098>.)
- U.S. Army Corps of Engineers, 2002, Dredged material management plan and environmental impact statement, McNary Reservoir and Lower Snake River Reservoirs: U.S. Army Corps of Engineers, Walla Walla District, Hydrologic Analysis, appendix A, 27 p.
- U.S. Geological Survey, 2006, Collection of water samples (ver. 2.0): U.S. Geological Survey Techniques of Water-Resources Investigations, book 9, chap. A4, accessed November 8, 2008, at <http://pubs.water.usgs.gov/twri9A4/>.
- U.S. Geological Survey, 2012, Annual water data report for water year 2011: U.S. Geological Survey database, accessed November 8, 2012, at <http://wdr.water.usgs.gov/wy2011/search.jsp>.
- Urick, R.J., 1975, *Principles of Underwater Sound* (2nd ed.): McGraw Hill, New York, 384 p.
- Wagner, R.J., Boulger, R.W., Jr., Oblinger, C.J., and Smith, B.A., 2006, Guidelines and standard procedures for continuous water-quality monitors—Station operation, record computation, and data reporting: U.S. Geological Survey Techniques and Methods, book 1, chap. D3, 51 p. (Also available at <http://pubs.usgs.gov/tm/2006/tm1D3/>.)
- Wall, G.R., Nystrom, E.A., and Litten, Simon, 2006, Use of an ADCP to compute suspended-sediment discharge in the tidal Hudson River, New York: U.S. Geological Survey Scientific Investigations Report 2006–5055, 16 p. (Also available at <http://pubs.usgs.gov/sir/2006/5055/>.)
- Wood, M.S., 2010, Evaluation of sediment surrogates in rivers draining to Lower Granite Reservoir, ID and WA—Proceedings of the 2nd Joint Federal Interagency Conference on Sedimentation and Hydrologic Modeling, Las Vegas, Nevada, June 27–July 1, 2010: Reston, Virginia, Advisory Committee on Water Information, CD-ROM, 12 p.
- Yellow Springs Instruments, 2011, 6-Series multiparameter water quality sondes user manual, rev. H: Yellow Springs Instruments, 377 p., accessed November 8, 2012, at <http://www.ysi.com/media/pdfs/069300-YSI-6-Series-Manual-RevH.pdf>.

This page left intentionally blank

Publishing support provided by the U.S. Geological Survey
Publishing Network, Tacoma Publishing Service Center
For more information concerning the research in this report, contact the
Director, Idaho Water Science Center
U.S. Geological Survey
230 Collins Road
Boise, Idaho 83702
<http://id.water.usgs.gov>



